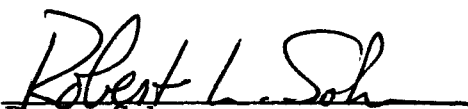5303-6014-TU000

STUDY OF UNMANNED SYSTEMS
TO EVALUATE THE MARTIAN ENVIRONMENT

Volume II. Experiments

Contract NAS 2-2478

23 September 1965

Submitted to

AMES RESEARCH CENTER

National Aeronautics and Space Administration

Moffett Field, California

R. L. Sohn
Study Director

P. Dergarabedian, Director
System Research and
Engineering Laboratory

TRW SYSTEMS, INC.

One Space Park

Redondo Beach, California

The present report is comprised of four volumes:

Volume I	Sensitivity Analysis
Volume II	Experiment Requirements
Volume III	Unmanned Spacecraft Design
Volume IV	Summary

FOREWORD

The principal authors of this report are:

Dr. C. D. Graves   (Nuclear Radiation Environment)

R. L. Sohn   (Mission Analysis, Meteoroid Environment)

T. Szekely   (Meteorology, Nuclear Radiation)

The contributions of Dr. R. S. Fraser to the meteorological system analysis are acknowledged.

TABLE OF CONTENTS

1. SUMMARY

Results obtained from the analyses reported herein are summarized below.

A numerical rating system for the experiment priorities was difficult to establish because basically different factors dictate the selection of the experiments, some based on design feasibility which tends to be either positive or negative without numerical differentiation, and others which are amenable to quantitative evaluation because bounds can be placed on the environmental factors involved and weight penalties estimated for design modifications necessary to accommodate the uncertainties. If bounds can be placed on the uncertainties, priorities generally can be reduced.

The priorities for the experiments in the order of their importance are: solar cosmic radiation environment, meteoroid environment, and atmospheric properties.

Because of uncertainties in solar radiation environment, shielding effectiveness, and man's tolerance to radiation, a comprehensive experiment program should be performed in earth-based facilities to establish shielding effectiveness and man's tolerance to the solar cosmic radiation environment. Recent data indicate that the recovery factor model (for repairable damage) developed for ionizing radiations may not be applicable to the types of radiations encountered in interplanetary space. Combining the uncertainty in the recovery factor with uncertainties in the environmental flux and effectiveness of shields (a factor of about 100 percent) leads to a possible weight penalty of about 9 percent. These uncertainties must be reduced prior to initiation of the Manned Mars Mission development program. A basically new approach to the measurement of the meteoroid environment must be established in order to acquire meaningful data for shielding design criteria. The approach to the measurement of the meteoroid environment proposed by TRW can yield data on the masses, velocities, and heliocentric trajectory characteristics of the particles, for sizes of particles applicable to the design of the manned system. This approach should be explored for application to precursor missions.

at two radio frequencies in order to determine the effects of near-surface ionization, if present; this measurement requires a second flyby probe mission. Alternatively, a small entry capsule could be ejected into the atmosphere, giving a relatively accurate fix on the density profile, and possibly an indication of the constituents. The latter experiment is preferred because of the greater confidence level in the results. Ultimately, landers should be deployed on the surface to give accurate data on pressure, temperature and constituents (through the use of a mass spectrometer).

2. INTRODUCTION

Volume I[1] summarizes the interaction of Martian and Cismartian environmental factors and the design and operation of the manned Mars mission spacecraft and excursion module. Estimates of the uncertainties in current definitions of the environment were made, and used as the bases for establishing possible increases in spacecraft gross weight, or additional complexities in mission operations. The degree of uncertainty could not be bounded for all environmental factors, and was treated parametrically where necessary to illustrate possible effects on the manned mission.

The present report establishes experiment programs for the measurement of environmental factors by unmanned precursor missions, based upon the results of the sensitivity analyses summarized in Volume I. Consideration was given to such factors as design feasibility, essential design criteria, system weight, mission operation, and system development. Numerical ratings only for each of these factors was not found to be adequate; "design feasibility," for example, cannot be assigned a relative numerical rating and compared vis-a-vis with "system weight," which is amenable to a quantitative rating technique. Hence, factors involving design feasibility were grouped in a high priority category with tentative numerical ordering within the category. This shortcoming, or lack of a "resolution," within the priority list is not expected to create a major problem in the selection of experiments for the unmanned precursor missions because the precursor spacecraft generally will have adequate payload capacity to accommodate most priority experiments.

A list of instruments was prepared, including physical descriptions, to accomplish the required experiments. This list is divided into groups according to mission mode requirements (interplanetary, orbiter or capsule/lander), and spacecraft weight capability.

2.1   R. L. Sohn, Ed., "Study of Unmanned Systems to Evaluate the Martian Environment - Volume I. Sensitivity Analysis," TRW Systems, Report 5303-6013-TU000. 23 August 1965. Contract NAS 2-2478

3. MISSION SCIENTIFIC ANALYSIS

3.1 Experiment Priorities

Volume I of the present report establishes the sensitivity of the manned Mars mission system to uncertainties in the Martian and Cismartian environment. These interactions were established by gathering and analyzing available data on the Martian and interplanetary environments, and placing upper and lower bounds upon the environment data in an effort to establish limits on the uncertainties in each environmental factor. (It was not possible to establish meaningful bounds on all environmental factors, and in some cases a parametric approach was used, that is, ranges of uncertainties in environmental factors were assumed and examined for the effect on mission system design.) A reference manned mission system design was selected based upon a design study conducted previously for the NASA Ames Research Center[1], and utilizing the Mars orbiting rendezvous mode, analogous to that being planned for the Apollo lunar program. The design was established for the opposition-class missions of approximately 14 months duration, and was capable of either aerodynamic or retro capture at Mars; chemical and nuclear propulsion systems were considered. Weight scaling laws were available for each of the designs so that the interactions of environmental factors on the system design could be readily evaluated in terms of overall gross weight in the earth parking orbit.

The designs were analyzed to determine the effects of uncertainties in the environmental factors on the system design, particularly in terms of the gross weight of the system. The matrix of environmental factors and system design elements for which interactions were considered is given in Table 3.1. The results of the manned mission sensitivity analysis are given in Table 3.2.

3.2 Priority Ratings

A numerical rating system was used to aid in establishing priorities for the measurements of the Martian and Cismartian environment factors. Each

---

1. R. L. Sohn, ed., "Study of a Manned Mars Landing and Return Mission." TRW/ STL Report 8572-6011-RU000, 24 March 1964. Contract NAS 2-1409

TABLE 3.1   MISSION-ENVIRONMENT INTERACTIONS

N - Numerical Analysis
Q - Qualitative Discussion
1 - To be analyzed in Phase II

| | MISSION MODULE | | | | | | MARS EXCURSION MODULE | | | | |
	Radiation Shield	Meteoroid Shield	Aero-Entry L/D	Aero-Entry Heat Shield	Orbit Alt.	Propellant Storage	Orbital Reconn	Radiation Shield	Meteoroid Shield	Aero Entry	Deceler
Atmosphere											
Thermodynamic Properties			N	N	N		Q			N	N
Density vs Altitude			N	N	N		Q	N	Q	N	N
Surface Density								N			N
Temperature vs Altitude				N							
Surface Temperature											
Chemical Composition			N	N						N	
Electrical Properties											
Ionosphere	Q				Q						
Diurnal & Seasonal Effects			Q^1	Q^1	Q^1					Q^1	N
Meteorology											
Winds							Q			Q^1	N^1
Cloud Cover							Q				
Dust Storms							Q				
Climate							Q				
Surface Conditions											
Surface Composition											
Soil Strength Properties											
Topography											
Radioactivity											
Areology							Q^1				
Biology - Vegetation							Q^1				
Radiation Environment											
Cosmic Radiation at Surface								N			
Cosmic Radiation - cismartian	N										
UV Radiation Density at Surface											
Van Allen Belt	Q^1				Q^1			Q^1			
Micrometeoroid Environment		N							Q		
General											
Reflectivity - Albedo						Q					
Magnetic Field	Q^1				Q^1			Q^1			
Gravitation Field					Q						

2

SURFACE OPERATIONS ⟶

...ator	Drift Sensor	Retro	Impact Gear	Propulsion	Propellant Storage	Rover Design	Traverse Range	Contamination Procedures	Experiment Program	Crew Effectiveness	Elec Equip Operation	Stay Time	Navigation	Devel Testing
	N	N	N	N	Q	Q			Q	Q			N	Q^1
	N	N	N	N									N	
	N	N	N	N	Q	Q				Q	N			Q
					Q									
					Q	Q				Q	Q	Q		Q
						Q			Q	Q	N			Q
	N	N	N	N	Q	Q			Q			Q		Q
	N^1	N	N^1						Q	Q	Q	Q		Q
	Q	Q				Q	Q		Q	Q		Q		Q
									Q					
					Q									
			N			N	N		Q					Q
			N			N	N		Q					Q
			Q			N	N		Q					Q
						Q			Q	Q	Q	Q		Q
						Q	Q^1		Q^1					
							Q^1	Q^1	Q^1					Q^1
						Q	Q			Q	Q	Q		Q
														Q
						Q			Q	Q	Q			Q
														Q
											Q			Q
													Q	Q

Table 3.2 SENSITIVITY ANALYSIS

C ARRIVE EARTH - AERO
A DEPART MARS - CHEM
C ARRIVE MARS - AERO
A DEPART EARTH - CHEM
% CHANGE IN EARTH ORBIT WEIGHT

	AERO AT MARS			RETRO AT MARS		FLYBY		DIRECT	
	CACA		NANA	CCCA	NNNA	CA	NA	CACA	NANA
	1982	1986							
UNCERTAINTY IN ATMOSPHERE									
CAPTURE	1.8	1.4	1.3	0	0	--	--	0.2	1.7
MEM	2.5	2.3	2.1	1.7	2.1			4.8	3.8
COMBINED	4.3	3.7	3.4	1.7	2.1	<1.0	<1.0	6.0	4.6
EFFECT OF WINDS									
50% WINDS (GRADIENT)	0.3(0.4)*	0.3(0.4)*	0.3(0.3)*	0.2(0.2)*	0.3(0.3)*			2.4(2.8)*	2.4(2.8)
MAX WINDS (NO GRADIENT)	0.3(0.2)	0.3(0.2)	0.3(0.2)	0.2(0.1)	0.3(0.2)			2.3(1.6)	2.3(1.6)
MAX WINDS (GRADIENT)	0.7(1.1)	0.7(1.0)	0.6(0.9)	0.5(0.7)	0.6(0.9)			5.6(8.0)	5.6(8.0)
MAX WINDS (GRADIENT, NO RANGE MAKEUP)	0.2(0.2)	0.2(0.2)	0.1(0.1)	0.1(0.1)	0.1(0.1)	<1.0	<1.0	1.3(1.2)	1.3(1.2)
MICROMETEOROID DOUBLE THICKNESS	7.5	5.4	4.8	8.9	10.1	14.6	7.9	21.4	20.8
MSC/STL (Cometary)	7.4	5.7	4.8	6.8	7.1	10.0	6.5	14.5	14.3
SOLAR COSMIC RADIATION HALF THICKNESS (90% RECOVERY)	-4.8	-6.5	-3.9	-6.5	-5.0	-9.1	-9.1	-5.2	-5.8
UNCERTAINTY IN SHIELD EFFECTIVENESS & FLUX	3.5	4.7	2.8	4.7	3.6	6.6	6.6	3.7	4.2
TOTAL UNCERTAINTY	8.3	11.2	6.7	11.2	8.6	15.7	15.7	8.9	10.0

* Sch Upper Limit

Table 3.3 ENVIRONMENT EVALUATION PRIORITIES

	DESIGN FEASIBILITY	WEIGHT PENALTY	OPERATIONAL CRITERIA	DEVELOPMENT CRITERIA	EXPERIMENT ACCURACY
ATMOSPHERE					
THERMO ⎫ PRESSURE ⎪ TEMPERATURE ⎬ CHEMICAL COMP ⎭	2	2	1	1	50%
ELECTRICAL PROP	–	2	–	–	
IONOSPHERE	–	2	2	–	
SURFACE IONIZATION	1	1	1	1	
DIURNAL AND SEASONAL EFFECTS	2	2	1	–	
METEOROLOGY					
WINDS	2	1	2	–	50%
CLOUDS	–	–	1	–	
DUST STORMS	1	1	1	–	
CLIMATE	1	–	1	1	
SURFACE CONDITIONS					
SURFACE COMP	2	1	2	2	
SOIL PROPERTIES	2	1	2	2	25%
TOPOGRAPHY	1	1	2	2	
RADIOACTIVITY	1	–	1	1	
SEISMIC ACT	1	–	–	–	
AREOLOGY	(SEE SURFACE CONDITIONS)				
BIOLOGY	2	1	2	2	
RADIATION ENVIRONMENT					
COSMIC RAD SURFACE	2	1	2	1 ⎫	20%
COSMIC RAD – CISMARTIAN	3	3	3	3 ⎭	
UV RAD AT SURFACE	1	–	2	–	
METEOROID ENVIRONMENT	2	3	1	1	60%
GENERAL					
ALBEDO – ABSORP	1	1	–	1	
MAG FIELD	1	–	–	–	
GRAV FIELD	1	1	1	–	

3 HIGH PRIORITY
1 LOW PRIORITY

Experiment	Quantity	Instrument	Mode
ATMOSPHERE			
1	Density vs height	Accelerometer trace during descent	Descent with data capsule. (Seif-type capsule, or any survivable lander).
2	Pressure and temp vs height	Static pressure and temp sensors	Same as (1)
3	Gas composition	Spectral radiometer	Same as (1)
4	Gas composition; pressure vs height	UV spectrometer (JPL 31)	Orbiter. Instrument pointed at Sun.
5	Gas composition; pressure vs height	IR spectrometer (JPL 32)	Orbiter. Instrument pointed at Sun.
6	Gas composition at surface	Mass spectrometer (JPL 6)	Lander. Instrument activated after landing.
CISMARTIAN RADIATION			
7	Galactic and solar cosmic particle flux	Particle flux counter. Multiple tubes with cascaded solid state detectors. (JPL 41 and 42).	Bus during transit. Orbiter at Mars.

TABLE 3.4   EXPERIMENTS SUMMARY

Data Capabilities	Physical Char		
	Weight (lbs)	Power (Watts)	Volume
edium accuracy data. Requires curate knowledge of entry angle. oncurrent data on pressure and mperature not accurately known itil subsonic portion of descent. ne-shot experiment.	1. 0		12 in^3
ensors accurate during subsonic escent - less accurate during eceleration. Required on nders.	0. 5		5 in^3
easurements in at least 4 avelengths	2. 0	10 (Items 1-3)	15 in^3
ata taken as atmosphere passes rough Sun-instrument line. epeated calculation necessary establish atmosphere model. aluable for measuring seasonal iriations and augmenting data ken during capsule descent.	22	12	9 x 10 x 12 in optics plus 6 x 10 x 6 in electronics
ame as (4). Data on constituents upper cloud structure which sorb in IR.	29	7	12 (Diam) x 15 in.
etermination of the composition f the atmosphere. Representa- ve samples of the atmosphere equired.	6	6	10 x 5 x 3 in.
rovide quantitative information bout direction, energy and types f particles. Primarily for very igh energy particles.	10	2	2 (Diam) x 15 in. (4 tubes)

.cteristics

Bits	Duty Cycle	Value
	Continuous during descent	3 (Valuable precursor experiment)
	Continuous during descent	
150/sec +7000 bits storage. (Items 1-3)	Continuous during descent	
5000 bits per sample.	One sample per orbit.	2 (Valuable adjunct to lander capsule experiment.)
5000 bits per sample	One sample per orbit.	1 (Adjunct to lander capsule experiment)
1100 bits per sample	12 per day	2
	Continuous	3 (Valuable to establish manned, shielding requirements)

Experiment		Instrument	Mode
8	Solar Cosmic particle flux	Particle flux (JPL 37)	Bus during transit. Orbiter at Mars
9	Solar cosmic radiation flux	Ion chamber (JPL 38)	Bus during transit. Orbiter at Mars.
10	Trapped radiation at Mars	Trapped radiation detectors (JPL 39)	Orbiter at Mars. Eccentric orbit required with high inclination to equator.
11	Magnetic field	Magnetometer (JPL 36)	Bus during transit. Orbiter at Mars.
SURFACE RADIATION			
12	Solar cosmic radiation flux at Mars surface	Ion chamber (JPL 38)	Lander
13	Light intensity at Mars surface	Photometer	Lander
14	UV intensity at Mars surface	Photometer	Lander

2

TABLE 3.4 EXPERIMENTS SUMMARY

Data Capabilities	Weight (lbs)	Power(Watts)	Volume
Provide semi-quantitative information about energy and types of particles. Used in conjunction with ionization chamber	2.5	0.35	4 x 5 x 6 in.
Measure total ionizing radiation (cosmic rays) and variation with time and position in Earth-Mars transit.	1.3	0.10	6 in. sphere
Search for magnetically trapped particles in the vicinity of Mars. If present, to study their intensity, direction and spatial distribution.	4	0.7	4 x 5 x 5 in.
Establish the existence of a planetary field and to establish its characteristics: magnitude, direction, polarity and orientation. Investigate the nature of interface between planetary and interplanetary magnetic fields.	5	5	4 x 4 x 6 in.
See (9)	1.3	0.10	6 in. sphere
Measure light intensity	0.5	0.10	1 x 1 x 2 in.
Measure UV intensity	0.5	0.10	1 x 1 x 2 in.

.cs

Bits	Duty Cycle	Value
	Continuous	3 (Valuable to establish manned shielding requirements)
	Continuous	3 (Adjunct to particle flux experiments, (7) and (8).
	Continuous	3 (Valuable to establish parking orbit altitudes, shielding requirements, etc.)
24	One sample per minute	3
	Continuous	3
	One sample per hour.	1
	One sample per minute.	2

Experiment	Quantity	Instrument	Mode
15	Ionosphere	Measure electron density	orbiter
16	Surface ionization layer	Conductivity	Lander
METEOROID ENVIRONMENT			
17	Micrometeoroids (Interplanetary)	Micrometeoroid detector (JPL 46)	Bus during transit orbiter at Mars.
18	Meteoroids (Interplanetary and at Mars)	Pegasus-type space-craft	Pegasus (modified)
19	Meteoroids (Cismartian)	TRW UV detector	Orbiter at Mars.

2

TABLE 3.4 EXPERIMENTS SUMMARY

Physical Chara

Data Capabilities	Weight (lbs)	Power(Watts)	Volume
Sensor deployed on ship	9	1.5	40
Measurement of velocity and cumulative mass distribution of cosmic dust. This experiment is of little use for manned precursor missions because size of particles detected are insignificant.	8	0.5	10 x 10 x 6 in.
Measurement of number of hits. Indirect measurement of mass. Basically new approach to detection required in order to assess flux, velocity, mass and direction of particles. Large area surface required (at least 10,000 sq ft).		(No detectors currently avai	
UV detectors measure number, projected velocity and direction, and mass of meteoroids entering martian atmosphere. Huge volume of atmosphere results in many hits of significant particle size (milligram to gram). Use of two satellites enables velocity and direction of particles to be determined. Experiment can be incorporated on Voyager-type orbiter; separate Pegasus-type vehicle not required. .	5	1	

| Data Capabilities | Weight (lbs) | Power(Watts) | Volume |

cteristics

Bits	Duty Cycle	Value
30/sec	Continuous	
	Continuous	-- (Size of particle detected in-significant)
		3 (Valuable to establish meteoroid shielding re-quirements)
lable.)	Continuous	3 (Valuable to establish meteoroid shielding re-quirements)

Experiment	Quantity	Instrument	Mode
METEOROLOGY			
20	Clouds and dust	TV Camera	Orbiter
21	Winds (at surface)	Hot wire anemometer	Lander
22	Winds (at altitude)	Balloon with transmitter	Lander
23	Surface temperature map	IR radiometer (JPL 34)	Orbiter
SURFACE CONDITIONS			
24	Topography	TV camera	Orbiter. Low-altitude polar orbit preferable.
25	Topography	TV camera	Lander. During descent and after landing.
26	Surface properties	Soil mechanics experiment (JPL 24)	Lander.

TABLE 3.4 EXPERIMENTS SUMMARY

Data Capabilities	Physical Charact		
	Weight (lbs)	Power (Watts)	Volume
Record cloud formations. Record dust clouds. Can be combined with Item (20).	17	10	180 in^3
Measurement of surface winds (magnitude and direction).	1	0.1	200 in^3
Measurement of winds at altitude. Requires radio tracking from lander. One shot per balloon. Marginal amount of data for weight and complexity. No suitable alternatives.	16 - 20	< 1	18-20 ft dia
Thermal mapping of surface (also cloud tops). Measurement of atmosphere thermal balance; albedo.	3	3 3	5 x 7 x 4 in.
Map surface. Wide-angle and narrow-field optics desirable.	17	10	180 in^3
Detailed surfave map around landing wite. Similar to Surveyor.	(Similar to Item (24)).		
Measurement of load bearing strength, cohesive modulus, frictional modulus and bearing stability.	13	3	12 (Diam) x 24 in.

3

eristics

Bits	Duty Cycle	Value
8×10^5 per frame.	Limited by Mars-Earth communication link capacity	1 (Valuable for dust cloud information)
9 per cycle	One per 5 minutes	2
	Continuous	1 (Of less importance than surface winds).
8 per sample	Continuously every 10 sec.	2
8×10^5 per frame	Limited by Mars-Earth communication link capacity.	3 (Valuable to select landing site, supplement bio/geo experiments, etc.)
		3 (Valuable for surface operations, etc.)
10^3 total	Desirable to move to several locations.	2 (Valuable for surface operations).

Experiment	Quantity	Instrument	Mode
27	Seismic activity	Seismograph (3-axis) (JPL 26)	Lander
28	Surface composition.	X-ray diffractometer (JPL 22)	Lander
29	Surface composition.	Core and mill	Lander
BIOLOGY			
30	Cell growth	Cell growth multiple chamber (JPL 20)	Lander
31	Turbidity and pH growth.	(JPL 19)	Lander

2

TABLE 3.4 EXPERIMENTS SUMMARY

Data Capabilities	Weight (lbs)	Power (Watts)	Volume
Study of the internal activity and heterogeneity of Mars.	8	1	9 (Diam) x 6 in.
Identification of minerals and determination of relative quantities and precise composition of mineral assemblages.	10	15	10 x 10 x 10
Prepare subsurface samples for analysis.	30	300	1200 in.^{3}
Multiple biochemical laboratory capable of performing reactions characteristic of biological life. Used to measure ensymatic hydrolysis using fluorescent technique. Capable of carrying out growth and control experiments.	4	2	N/A
Changes in optical density and other light-scattering phenomena plus changes in pH are used to detect growing organisms in a transparent liquid culture media.	4	1	6 x 6 x 6 in.

eristics

Bits	Duty Cycle	Value
20 cps	Continuous	2 (Adjunct to surface conditions experiment, etc.)
5×10^4 per sample	Several samples and sites desirable.	2 (Adjunct to surface properties experiment, etc.)
5×10^4 per sample	Several samples and sites desirable.	1
100 per sample. 2250 bits per 12 hours.	Maximum possible.	3 (Valuable to establish quarantine and contamination criteria, etc.)
7 per sample.	Twice per hour, continuously.	3

The approximate physical properties of the experiments are given in Table 3.4, and the mode of operations (interplanetary bus, orbiter, descent capsule, or lander) is stipulated for each experiment. A numerical rating is given for each experiment to indicate its importance with respect to the design of the manned Mars mission system. Discussions of the requirements and technical approaches for the high-priority experiments are given in Section 4 to 7.

3.4 Mission Payloads

The following section presents a summary list of experiments for the various precursor mission modes, including flyby probes, orbiters and landers. The experiment payloads are compared to several possible launch vehicle payload capabilities, including the Atlas Centaur, and Saturn IB-class launch systems. A more detailed analysis of the experiment payloads and launch vehicle capabilities is given in Volume III. The technique used in matching the payload requirements with the launch vehicle capabilities generally follows the procedure outlined in the following section.

The various mission modes available for the unmanned precursor flights include the following:

o   Flyby
o   Flyby plus capsule/lander
o   Orbiter
o   Orbiter plus capsule/lander

For present purposes the direct lander systems are not considered.

The various mission options are reviewed in Volume III to indicate the most effective means of accomplishing the experiment goals. Because of small payload weights many of the high-priority experiments can be repeated on many missions to Mars. For example, measurements of the solar cosmic radiation environment will be repeated on all missions to the planet, thus, building up the necessary volume of data to develop statistically meaningful models of the solar cosmic radiation environment.

The summary list of experiments is presented in Table 3.6 in the order of the priorities established on the sensitivity analysis of the manned Mars mission. The experiments are grouped by mission mode. The weights for each experiment are tabulated, and the accumulated payload weights obtained by summing the experiments in the order of their priorities.

As indicated previously, it is possible to accommodate many of the high-priority experiments with a moderate total payload weight, such that it is possible to accomplish these experiments with an Atlas Centaur launch system. The Saturn IB-class launch system is required only for heavy landers. The high-priority experiments on the interplanetary bus/orbiter systems constitute a basic experiment package that probably can be incorporated on all missions to Mars.

The essential data on the atmosphere of Mars can be obtained by four different modes: by radio occultation measurements, by the use of ultra-violet and infrared spectrometers onboard the orbiting spacecraft (and by Earth-based IR spectroscopy), by the use of a very low weight, elementary entry capsule, and by a lander system of moderate weight. One or both of the latter modes is required in order to build up sufficient confidence in the definition of the atmosphere, particularly to include the diurnal and seasonal variations in the properties of the atmosphere; however, the degree of accuracy in the measurement of the atmosphere required for present purposes does not seem to justify lander experiments. The measurements made from the orbiter generally require that a model of the atmosphere be hypothesized so that the data obtained from the spectroscopic or occultation experiments can be introduced into the model in order to iteratively arrive at an agreement between the measurements made by the spectrometers and the hypothesized model. Because direct measurements of the atmosphere are not possible from the orbiter, the data acquired from the orbiter must

Table 3. 6   PRELIMINARY SCIENTIFIC PAYLOAD LIST

BUS/ORBITER

	RATING	WEIGHT (LBS)	WEIGHT SUMMATION (LBS)
PARTICLE FLUX (HIGH ENERGY	3	10	10
PARTICLE FLUX	3	2.5	12.5
ION CHAMBER	3	1.3	13.8
TRAPPED RADIATION DETECTOR	3	4	18
MAGNETOMETER	3	5	23
METEOROID ENVIRON. (STL)	3	5	28
MICROMETEOROID ENVIRON	3	8	36
TV	3	17	53
UV SPECTROMETER	2	22	75
IONOSPHERE EXP	2	3	78
IR RADIOMETER	1	3	81
IR SPECTROMETER	1	29	110

DESCENT CAPSULE

ACCELEROMETERS	3	1.0	1.0
PRESSURE, TEMP	3	0.5	1.5
GAS COMPOSITION	3	2.0	3.5
TV	3	15	18.5

LANDER

SOLAR COSMIC RADIATION	3	1.3	1.3
CELL GROWTH	3	4	4.3
TURBIDITY AND PH	3	4	8.3
TV	3	17	25.3
MASS SPECTROMETER	2	6	31.3
ANEMOMETER	2	1	32.3
UV DETECTOR	2	0.5	32.8
SURFACE IONIZATION	2	1.5	34.3
SURFACE PROPERTIES	2	13	47.3
SEISMOMETER	2	8	55.3
VISIBLE INTENSITY	1	0.5	55.8
X-RAY DIFFRACTOMETER	1	10	65.8
CORE AND MILL	-	30	95.8

be augmented with capsule measurements in order to establish a sufficient confidence level in the model. The direct measurements can be made by means of the descent capsule of the type proposed by Sieff of NASA Ames (and by a minimumly instrumented lander system which is capable of measuring the atmospheric properties in the vicinity of the surface of the planet). The descent and lander experiments can be accomplished with one lander system, of course.

The spectrometer systems aboard the orbiter are particularly useful for measuring properties of the upper atmosphere, including variations in these properties throughout the Martian day and Martian seasons. The infrared spectrometers can obtain information about the structure and composition of the clouds in the Martian atmosphere.

In summary, the definition of the atmosphere made by the orbiter experiments in itself is not adequate and must be augmented by additional measurements made from capsule/lander based experiments to define the atmosphere with sufficient accuracy.

All of the experiments listed can be achieved with moderate experiment payload weights, with the exception of the X-ray diffractometer, particularly if the experiment is serviced by the core and mill sample preparation equipments. This experiment, of course, is of interest to the scientific community, but is of lesser importance to the design of the manned lander system. Likewise the incorporation of balloon systems aboard the lander to measure the properties of the atmosphere at altitude, and in particular to measure the wind structures in the upper atmosphere, appears to be of marginal value when compared to the weight and complexity introduced into the spacecraft systems. Serious consideration should be given to these marginal experiments before they are incorporated into the lander payloads, particularly for the initial unmanned precursor missions. Careful attention must be given to the photographic mapping exercises performed both from the orbiter and lander craft. The mapping exercises are of extreme importance both for the scientific studies of the planet as well as to the gathering of important topological information necessary to select landing sites for the initial manned Mars missions. In fact, photographic surveys of the planets may in fact be given the highest priorities during the unmanned precursor missions. However, it should be noted that the photographic mapping experiments dominate the spacecraft data gathering, processing and transmission requirements, and must be carefully planned so that excessive

requirements are not placed upon the precursor missions. Selective mapping must be considered.

A good deal more consideration must be given to the biological experiments which are to be used to establish the contamination constraints upon the manned lander crews. Precursor experiments alone are not adequate to define bio-contamination hazards, and crew decontamination procedures have been established to serve such purposes in the absence of conclusive data from precursors (see Volume I, Section 10).

Discussions of specific experiments are given in the following sections.

4. NUCLEAR RADIATION ENVIRONMENT EXPERIMENTS

Experiments are proposed for the unmanned precursor mission(s) to obtain a better understanding of all the environment-dependent radiation particles and energy spectra that would be encountered in a Mars mission. Following the reduction of data from these experiments, shield design studies and experiments may be conducted (on earth) through the use of particle accelerators to determine shield geometries, shield materials, and shield methods (e.g., use of "biowells") to ascertain requirements imposed by:

1. Primary particles and their energy spectra, as well as event cycles and intensities.

2. Nature and spectra of secondary radiations produced by the interactions of the primaries with spacecraft and shield materials.

3. Nature and relative effects of biological damage to specific tissues and organs as related to exposure and shielding against specific particles and particle energies and fluxes of certain vital organs as well as whole body exposures (tissue-equivalent dosages). It is expected that biological dosage threshold values will be better defined as knowledge and understanding is obtained in this important area in the next decade.

4. Recovery effectiveness of the crew after exposure to representative radiation environments.

A preliminary list of these experiments is reported. This listing is predicated on the assumption that current and planned space radiation environment and biological effects experiments will continue for the next decade, supported by and coordinated with the proposed experiments program.

4.1 Interplanetary Radiation Measurement

During the transit to Mars for unmanned exploration a radiation experiment for monitoring the cosmic ray and solar flare protons is necessary. A typical instrument suitable for this measurement would be a combination solid state detector and scintillation counter. With this type of instrument

protons of energies from 4 Mev to 1 Bev can be measured, and both the intensity and energy spectrum of solar flare protons can be determined. An instrument of this nature would weigh approximately 4.5 lbs, would consume about 1.5 watts of power and require approximately 200 in^3 of volume. The typical sampling rates of this experiment would be 1 sample every 10 minutes for cosmic rays and 1 sample every 15 seconds during solar flares. Each sample would require about 13 bits of information.

4.2   Radiation Belt Measurements

It is not known at this time whether Mars has a radiation belt. In the event that Mars has a radiation belt, it will most likely be similar to the Earth's Van Allen belt. A typical instrument for measuring trapped radiation would consist of a telescope made up of 2 solid state detectors and a plastic scintillator. By judicious use of coincidence, anti-coincidence and pulse height analysis the following properties of the radiation can be measured:

1.   Electron flux in the energy range from 50 Kev to 5 Mev.

2.   Proton flux in the energy range from 10 Mev to 200 Mev.

3.   The energy spectrum of electrons in 15 channels with the electrons having energies greater than 2 Mev falling in the highest channel.

4.   The energy spectrum of protons in 16 channels with the energies greater than 100 Mev falling in the highest channel.

The instrument would be subcommutated through various operation modes to determine the energy spectrum and intensity of both electrons and protons. A total of approximately 150 bits would be required for a complete analysis and the analysis should be repeated approximately once per minute. The weight, power and environment requirements would be similar to the interplanetary instrument described above.

4. 3   Surface Radioactivity Measurements

On the first unmanned lander mission to Mars the surface radioactivity
should be measured. This activity could be induced by radioactive decay
in surface materials, by X-rays and by solar flare protons as well as
secondary neutrons produced in the atmosphere and impinging on the
Martian surface. A measurement of the resulting alpha, beta and gamma
radiation should be made. An instrument using solid state detectors can be
used for the alpha and beta measurements while a CsI scintillator would be
appropriate for gamma ray detection. The data rate would most likely be
very low (on the order of a few bits per minute) and weight, power and volume
requirements would be similar to the interplanetary radiation measurements
described above.

5. METEOROLOGY

Preliminary results are reported for a brief study that was addressed to consider meteorological experiments that are appropriate for assignment to an unmanned, soft-lander Mars mission that has as its purpose the accumulation of specific Martian environment data in a precursor mission(s) necessary to enhance the design of a manned Mars mission system.

5.1 Requirements from Meteorological Experiments

Atmospheric data regarding wind velocities, temperatures, pressures, composition and dust storms are required to establish

1) Propulsion and configuration design parameters for landing and boost take-off modes ($\angle V$, footprint, etc.).

2) Lander (excursion module), ground station, and pressure suit design parameters.

3) General system design definitions based on meteorological constraints unique to the Mars environment.

5.2 Meteorological Experiments System - General

Based on weight economics and on considerations involving continued system application beyond the unmanned precursor initial-experiment/data acquisition phase, an evolutionary meteorological system is proposed. This system would use

1) A polar orbiting satellite at a 600 n. mile altitude; this satellite would be a communication link between the surface-based and air-borne experiments and earth.

2) A weather-base ground station(s) deployed from the orbiter.

3) Instrument-bearing constant altitude superpressure balloons that would be deployed from the ground station(s) to float at pre-selected altitudes to sense atmospheric temperature, pressure and to be used for accumulating data on winds aloft.

4) Communication linkage between the balloons, ground stations and satellite to provide wind and atmospheric data as a function of geographic location and time (day, night, and seasons).

5) Tracking sensors aboard the orbiting spacecraft to measure balloon drift due to winds.

5.3 Ground Station

Surface Pressure

Conventional aneroids may be employed. Accuracy for pressure measurements from 0.10 to 0.30 mb are within state-of-the-art. Calibration is required for temperature effects. Accuracy improvement is achieved by reducing the expansion/contraction scale (strain gage) to expected surface pressures; hence three aneroids should be provided, one each for the three theoretical model atmosphere surface pressures of 40 mb, 25 mb, and 10 mb. For protection against excess loads and sudden pressure changes, the aneroids should be contained in sealed containers at their nominal pressure values; the seals would be punctured with a command signal following deployment.

Each barometer, together with its sealed container and electrical pickup would weigh approximately 0.3 pounds.

Atmospheric Surface Temperature

Redundant temperature measurements may be obtained from employing

1) A small metalized bead thermometer

2) A calibrated thin wire

3) A bimetallic thermal strip

The bead thermometer and thin wire are relatively insensitive to radiation-induced errors (during both daytime and nighttime hours) even when modest ventilation provisions are made. However, the small bead suffers from self-heating when in a measurement circuit, and the thin wire requires an elaborate electronic circuit to permit accurate telemetry. A sophisticated circuit design may be employed to reduce the self-heating effect on error in the bead; accuracy to less than $1^{\circ}C$ has been obtained with elaborate circuit designs employed with bead thermometers.

For the three thermometers and their associated electronic circuitry a total weight of 1 pound is estimated.

Wind Velocity and Direction

For wind surface measurements a conventional light-weight anemometer and wind vane may be employed. The anemometer may use aluminum and plastic cups and the wind vane may be an aluminum airfoil. The anemometer and wind vane require vertical positioning at an altitude of about 2 meters above the ground station; this vertical position may be obtained by employing a set of gimbal rings and a counterweight. The axis of the anemometer and wind vane would pass vertically downward through the gimbal ring set and into the counterweight (made up of battery and electronic components).

To provide a reference for wind direction a set of equal-spaced solar cells may be provided on the periphery of a vertical cylinder that is concentric with the wind vane axis. Sun direction would be determined at any time with the solar cell that has maximum output; the angle between this cell and the wind vane direction would be obtained with an appropriate electrical pickup and circuitry. Total wind vane and anemometer system weight (without the battery and electronics counterweight) is estimated at 10 pounds.

Atmospheric Electrical Conductivity

To provide information on atmospheric conductivity and to enhance the design of electronic systems operating in the martian environment without arcing out, conductivity measurements are required. A weight of 0.5 pounds is estimated for this experiment.

Surface Dust Measurements

An acoustical-microphone pickup may be mounted rigidly on the leading edge of the wind vane so it is normal to the wind at all times. This pickup would be calibrated to measure impacts from dust particles. A weight of 0.5 pounds is estimated for this experiment.

Additional acoustical pickups may be placed adjacent to each solar cell that is mounted on the periphery of the vertical cylinder that is used for obtaining the sun angle. An additional weight of 1.5 pounds is estimated for the microphones and circuitry.

Atmospheric Molecular Weight

A calibrated balloon-release spring may be provided along with

electrical pickup to read the buoyant force of an inflated weather balloon (prior to release). Knowing the ambient temperature, ambient pressure, balloon volume and mass (for super-pressure, constant-volume balloon), the balloon payload mass, and the spring constant of the release spring (calibrated for temperature), the atmospheric molecular weight can be calculated.

5.4   Weather Balloons

Super-Pressure Balloons

The present technology of balloon developments has reached a point where unballasted balloons weighing approximately one kilogram will remain aloft on Earth for periods of several months, floating at constant density altitudes. These weather balloons, designed to carry instrument payloads, use either thin-film or miniaturized electronic circuits; the miniaturized circuits appear to show more promise for reduced weights. Present global weather programs (e.g., GHOST) consider the use of such balloons together with satellite surveillance techniques to determine their location at suitable intervals. By computing their direction and rate of motion, they can provide wind information as well as temperature and other parameters (pressure, humidity, ozone content, etc.) to the satellite. These super-pressure balloons can fly to altitudes as high as 10 mb pressure on Earth.

The super-pressure balloon has many advantages over zero-pressure balloons which require from 5 to 10 percent additional weight as ballast that must be dropped to maintain altitude. For flight requirements exceeding approximately two weeks an unreasonably excess ballast weight is required. Largely sponsored by ONR developments in 1957-1960, Mylar spherical balloons have been made without an appendix so that free lift introduced on the ground is converted to super pressure at flight altitude. Assuming a tight and unyielding balloon material, the overpressure equals the free lift plus superheat. When the gas cools the overpressure decreases but remains positive. Since mass and volume are unchanged the balloon continues to float at a constant density-altitude without ballast.

Considerable information has been obtained about seals, pinholes and

necessary overpressures to overcome day-night and infrared radiation fluctuations. Basic advances have been made in development of strong "bi-tape" seals on both sides of the balloon gore as well as on the use of bi-laminated Mylar film to eliminate leaks caused by small pinholes in the cast film. Super-pressure balloons can presently be made of laminated Mylar gore in sizes from 4 feet to 120 feet diameter and will withstand stresses in excess of 1000 psi at test temperatures as low as -60°C. At present these advances enable earth flights with 120 foot (diameter) balloons carrying up to 300 pounds of payload.

In April and May of 1964, NCAR launched several balloons (from Japan) that were designed to float at 200 mb pressure altitude. Staying aloft for six to ten days, these balloons carried a 240 gram payload and, because they carried no storage cells, were active only in the daytime. Using thin-film or microelectronics, it appears from GHOST program study results that this payload weight may be reduced to 80 grams. RCA has developed a lightweight transmitter weighing only 60 grams and producing 5 watts at 5 megacycles. Using a solar cell power supply taken at 0.3 gm/cell a total solar cell weight of 60 grams would appear adequate as an energy source (300 milliwatts) for a low-powered balloon electronics system on the planet Mars. Interrogation would be largely confined to daylight hours, but lightweight storage cells may be added to permit short period night-time interrogations; an additional 300 grams would be added (reduced from the instrument package).

Martian Atmosphere Balloon Study Results

Assuming a Mean* Model Standard Atmosphere of 25 mb surface pressure, along with the assumptions that:

Molecular Weight	-	29.7
Surface Temperature	-	250°K
Troposphere Lapse Rate	-	-3.89°K/km

---

* Model 2 in Table 5.5 on Page 5-10 in Quarterly Progress Report No. 2, TRW/STL 5303-6007-TU000, "Study of Unmanned Systems to Evaluate Martian Environment," 31 March 1965.

of 5000 and 20,000 feet. These results are shown in Table 5.1. As indicated in the table, balloon diameter and weight are more sensitive to payload requirements than to altitude (unlike on Earth where the atmospheric pressure gradient is steeper than that of Mars). Payload weights of 0.5 pounds and 4.14 pounds were assumed. The weight of 0.5 pounds assumes an extremely optimistic electronics development program and a very modest experiment system. The heavier payload of 4.14 pounds is based on the results from the balloon instrumentation study made in the next section.

Table 5.1

MARTIAN WEATHER BALLOON SYSTEMS

Altitude, ft	5000	20,000	20,000
Balloon Diameter, ft	18.00	21.00	28.00
Mylar Weight (includes support netting), lb	5.50	7.45	14.719
H_2 Weight, lb	0.45	0.58	1.364
Balloon Payload Weight, lb	0.50	0.50	4.140
Total Balloon and Payload Weight, lb	6.45	8.53	20.223
H_2 Supply Tank, lb (Spherical titanium tank at approx 2000 psi storage pressure)	7.87	9.70	23.00
H_2 Supply Tank Regulators and Attachments, lb	1.50	1.50	2.00
TOTAL Weight of Equipment, lb (For launching 1 balloon)	15.82	19.73	45.223

Balloon Instrumentation

Following a review of development feasibility evaluations for the use of lightweight microelectronic circuit systems for the GHOST and IRLS programs, preliminary payload weight estimates have been made for the balloon experiments. These preliminary weight estimates are shown in Table 5.2.

Table 5. 2

BALLOON INSTRUMENTATION PAYLOAD ESTIMATE

		Weight (Grams)
Instrumentation		200
Metalized bead thermometer (0.4 mm dia.)	100	
Aneroid barometer (strain gage transducer)	100	
Power and Electronics		1675
Solar Cell and cell assembly	120	
Thin-film battery	350	
Electronics and antenna	800	
Transmitter (10 watts, 0.1% duty cycle 210 milliwatts avg. power)	55	
Receiver (pulsed standby operation, 250 mw avg. power)	50	
Peak power storage cell for transmitter (for night-time operation)	300	

TOTAL   1875 grams
                              (4.14 pounds)

5.5 Satellite

If a single polar-orbiting satellite is employed in a circular orbit at 600 miles altitude it will have a period of 114 minutes/revolution. With a radio range of approximately 1350 miles, and for a position over the martian equator where the frequency of interrogation-possible overpasses is at a minimum (maximum over the poles), it is possible to make an average of 2.26 interrogations per day. For a maximum wind velocity of 200 feet/second at a balloon altitude of 20,000 feet (Model 2 Martian atmosphere, assuming a gradient increase of 4 feet/second wind velocity per 1000 feet of altitude), the balloon may drift as far as 1632 miles/day and the maximum expected position change per interrogation will be 722 miles (at the equator, where the least interrogations/day are encountered); this will be within the communications range of the satellite and there will be no "balloon loss."

For any satellite with orbit inclination less than for the polar orbiter, the communication range requirements (to assure no "balloon loss") can be reduced; the equatorial orbit would have a minimum range requirement (for near-equatorial balloon locations).

While the altitude for a synchronous equatorial satellite is less for Mars than for Earth (9800 n. miles versus 20,000 n. miles for Earth), this altitude may tax the communication power requirements; also longitudinal drift and position-keeping propulsion requirements would add to the satellite weight. For these reasons and because the synchronous satellite would not provide global coverage and would restrict surveillance positions to equatorial areas, the synchronous satellite is not recommended for initial experimentation.

The satellite is basically a data handling and communication device. It provides a ranging and telemetry link from the ground station and floating balloons, and a read-out link to Earth. For the meteorological experiment data and including satellite-to-ground TV operation, assuming the use of six balloons deployed from the ground station (at preselected intervals and to different altitudes), the solar cell power requirement for the satellite will be approximately 2/3 that of the present Nimbus satellite and the number of solar cells approximately the same as on Nimbus.

5.6   Satellite-Balloon Communication System

Many recent studies have been made on satellite earth surveillance systems that use balloons for wind velocity (range) and upper atmospheric parameters (temperature, pressure, etc.) measurements. In a proposal by J. E. Blamont for the EOLE experiment,* a satellite serves as a buffer memory as it interrogates and records the information telemetered by automatic balloon and buoy (sea surface) stations. This satellite then communicates the data to specific ground data handling stations. This approach is taken after the "Interrogation, Recording, and Location System," an experiment on the Nimbus B spacecraft scheduled for launch

---

*   Centre National d'Etudes Spatiales de France

early in 1967. * For the IRLS experiment, the satellite will collect data and permit determination of each station location in terms of its latitude-longitude coordinates, thus enabling the tracking of super-pressure balloons and plotting of upper atmosphere wind fields. A similar system but with less numbers of balloons is proposed for the meteorological experiments on Mars.

The satellite-balloon location and interrogation system would operate to:

1) Interrogate one particular balloon among several balloons present in the observation range of the satellite

2) Measure the satellite-to-balloon range with adequate accuracy (on the order of approximately 1 km)

3) Transfer meteorological data obtained from the balloon into the satellite memory

4) Enable multiple data read-out from the satellite memory to Earth-based ground acquisition stations.

Interrogation and Recording

To permit communication with any specific balloon, each balloon (and ground-based station) is assigned a discrete address. The interrogation command, through an assigned command word, provides the address of the balloon to be interrogated and the exact time (referenced to satellite orbit time), that the balloon is to be interrogated. A very stable clock is employed by the spacecraft to control the time of execution of critical operations throughout any one orbit and to keep track of time in the orbit relative to a starting time. The starting time is reset to zero when the Earth-based station communicates with the satellite. (In the IRL system, a counter, synchronized by the Nimbus clock, is used to develop a 16-bit code word corresponding to the orbit time relative to zero and is updated each second of real time. The coding arrangement is simple binary coding and corresponds to the coding arrangement of each command word; thus a means is achieved for developing a time code in the satellite which can be compared to any time code in an interrogation command word.

---

*"WA 6.1: The Interrogation, Recording and Location System Experiment," by J. R. Cressey and G. D. Hogan of NASA/Goddard SFC. (Proceedings of the 1965 National Telemetering Conference, 1965 Instrument Society of America--APR. 14/9:00-12:00/Bluebonnet).

Responding to the interrogation command, the proper balloon turns on its dormant circuits, including its transmitter, and encoded data (measured parameters of temperature and pressure) are transmitted to the satellite. The satellite stores these data for subsequent readout to the earth station. The amount of data stored during any single orbit (or multiple number of orbits) is a function of the number of balloons and ground-based stations interrogated, the numbers of data points and the resolution of the digitization at the balloon and ground-based stations.

Range Measurement and Balloon Location

Ranging

Range between the satellite and balloon is obtained by determining propagation time of an RF signal (sent from the satellite and returned by the balloon transponder at a different carrier frequency) through phase lag between the satellite clock and the signal received from the balloon. The satellite measures the time delay between the leading edge of the trans-mitted signal and the leading edge of the returned signal. This gives a rough range estimate between the balloon and satellite. Next, the satellite makes a phase comparison between the transmitted and received sub-carriers. This is used to improve the accuracy of the range measurement. The satellite digitizes the range measurement and stores it, along with the address of the balloon and the time of the interrogation. After com-pletion of the ranging sequence the balloon switches to a telemetry mode and transmits to the satellite the meteorological parameters measured by the balloon. The satellite digitizes the telemetered information and adds this to the stored memory.

Providing that the satellite ephemeris is well-known, electronic ranging is the best approach to locating free drifting balloons with a single data collection system. The only real problem in the IRL satellite ranging system now under consideration for use in earth air/sea navigation and traffic control systems is the requirement to serve a network of buoys whose population and population density is large enough to detract from economic attractiveness due to expensive traffic control requirements.

Location*

The common intersection point of two spheres with the Martian surface would locate an interrogated balloon at a given moment. This, of course, is the simple case where the balloon immediately returns a pulse transmitted from the satellite on two consecutive occasions. The radii of the spheres are proportional to the propagation time of the pulses and the centers of the spheres are the positions of the satellite at the time the pulses are transmitted and received (see Figure 5.1).

Balloon location may also be obtained by using hyperbolic geometry, that is, the common intersection of two hyperbolic surfaces with the surface of Mars provides a locus. This method is only slightly different mathematically than that for the spherical case. A range difference measurement is determined from either (1) the satellite measuring the difference in arrival times of two consecutive pulses which were transmitted by the satellite and immediately repeated by the balloon, or (2) the balloon measuring the difference in arrival times of two consecutive pulses transmitted from the satellite and relaying the ranging information back to the satellite via the digital form. A range difference is used to generate a hyperbolic surface whose focal points are the positions of the satellite at the times the two pulses are received. For two hyperbolic surfaces sharing one focal point, only three pulses are necessary.

With only slight mathematical departure from the previous two methods, a third method may be used; this involves determining the common intersection of two elliptical surfaces. It is like the spherical concept except that the spheres become ellipsoids because the balloon delays its response (with a built-in clock) to the satellite an appreciable assigned amount of time to avoid interference with responses from neighboring balloons. The focal points of an elliptical surface are the positions of the satellite at the time when the pulse is transmitted and at the time when the pulse is received.

---

* "WP 10.3: Communication Traffic Control of a Buoy Network in a Satellite Data-Collection System," I. D. Smith, Raytheon Co., Sudbury, Mass. APR. 14/1:30-4:30/AZALEA, Proceedings of the 1965 National Telemetry Conference, April 1965

Combinations of these three basic positioning concepts might be employed; the method chosen depends on the way in which message traffic is controlled.
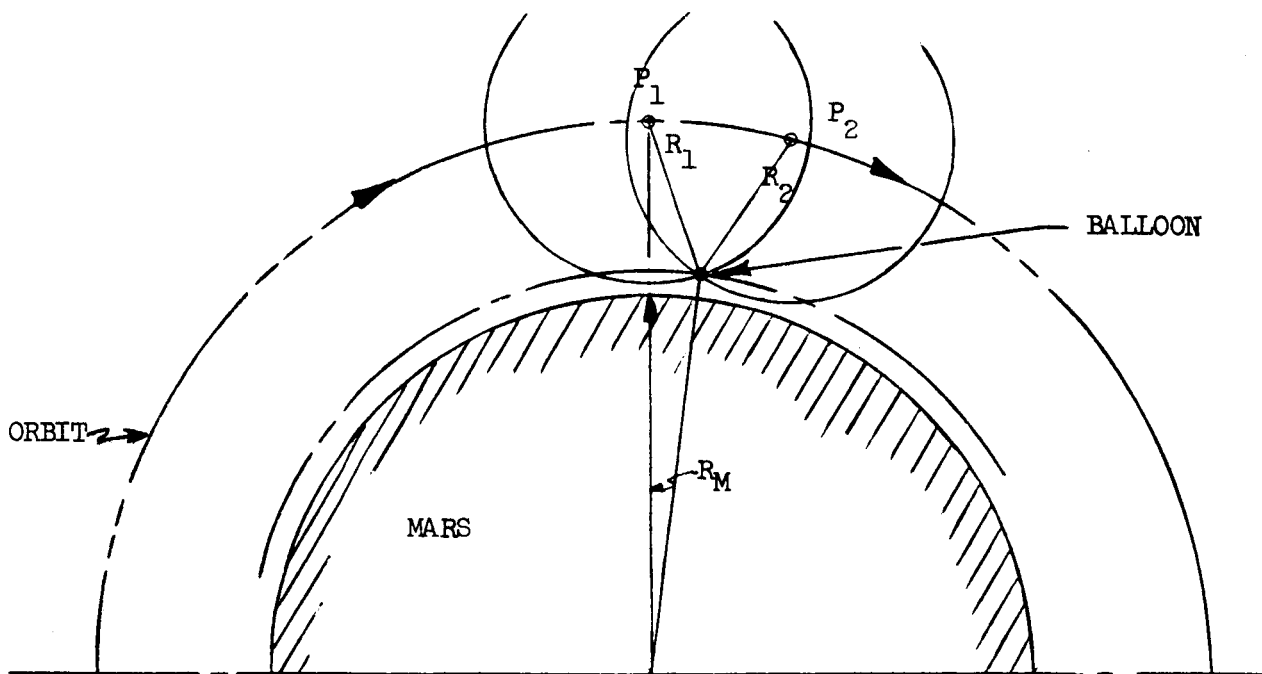

Figure 5.1   Balloon Locations by Sperical Solution

5.7 Satellite-Borne Meteorological Experiments

Additional meteorological experiments will be carried out from the orbiting satellite, primarily to analyze cloud cover, and to measure surface temperature patterns, albedo and atmosphere heat balance.

The amount of data gathered in connection with meteorological experiments should be carefully limited in accordance with precursor mission objectives, which are not aimed at comprehensive meteorological research, but at less detailed coverage designed to support the manned landings. Earth-based satellite weather programs are still in the early research stages and may remain so until a higher degree of utilization can be obtained from the large mass of photographic data gathered to date. The Mars precursor satellites cannot afford to support such an extensive data-gathering requirement because of the relatively low effectiveness of such data. The following comments briefly review present earth-based meteorological research.[1]

"The principal result of the Tiros photographs has been the demonstration that cloud formations form patterns on a global scale and that these patterns are sufficiently distinctive, enduring and meaningful to permit reliable weather forecasting. The Tiros photographs have shown, for example, that both extratropical and tropical cyclones are characterized by a vortex or spiral-cloud pattern about their centers. Moreover, each storm displays unique characteristics superimposed on the basic pattern so that a specific storm can be recognized and plotted some time before it could have been identified on the earth. The utility of nephanalysis (the analysis of these cloud patterns) in weather prediction has been proved as well in the recognition and tracing of cold fronts, large areas of stratus cloudiness, unstable areas, local storms and jet streams.

"Insight has also been permitted into the theoretical basis of the meteorological phenomena revealed in the photographs. The Tiros histories of typhoons and hurricanes have revealed a pattern evolution on the basis of which a correlation can be made with the surface maximum winds in the storm. By means of this technique it is possible to distinguish

---

[1] T. L. Branigan, Editor, "Space Log." TRW Space Technology Laboratories. Vol. 4. No. 4. Winter 1964-1965, p. 30.

in the photographs between hurricane and sub-hurricane stages of storm development and to calculate surface wind velocities with an accuracy of 25 percent.

Until the Tiros flights it had been assumed, at least as a first approximation, that cellular cloud formations were the result of vertical shear and horizontal winds on hexagonal Benard cells, i. e., those cells which form when a layer of fluid is heated from below so that convection forces the fluid to rise above the source of heat and fall back at a perimeter beyond the heat source. This theory called for a cloud width about three times the cloud height, but many patterns found by Tiros exhibited a nearly regular structure in which the width was approximately 30 times the height.

A partial explanation of the formation of cellular clouds now takes into account the eddy coefficients in the turbulent flow, that is, the horizontal components of the convection. In rotating cells, the rising air penetrates a short way into the stable layer above the base of the inversion. The airflow then moves horizontally in the stable inversion, finally to descend where the air is cloudless. Since the vertical component acts to reduce the differences in temperature and velocity between the horizontally moving air at the top and bottom of the cell, the vertical flow must operate across the inversion and is, therefore, kept relatively small. When the ratio of horizontal to vertical flow is about 100, which appears frequently to be the case, the cells can exhibit a flattening 10 times that predicted by the classic Benard cell explanation. In addition, it appears that baroclinic instability, the instability produced when isobaric and equal-density surfaces do not coincide, that is introduced by horizontal temperature gradients can produce flattened cells independently of the relative strengths of the vertical and horizontal coefficients. All of the significant factors will need to be combined eventually into a unified theory before the flattened cells of the Tiros photographs are fully explained.

Other theoretical results made possible by Tiros are the recognition and description of wave patterns in clouds resulting from the flow of wind over and perpendicular to large mountain ranges and of the spiral patterns formed in the lee of elevated islands. The photographs from space of Hurricane Anna in July 1961 served also to provide evidence verifying the theoretical explanation of the change in airflow associated with the onset of instability leading to hurricanes.

The relatively successful flight (marred by the failure to achieve the planned circular orbit) of Numbus 1 has provided a substantial improvement in the quality of data on which the meteorological research can be founded. The increased resolution of both visible and infrared coverage permits more detailed measurement of cloud height, a global investigation of temperature gradients in ocean currents, the thermal emission properties of various types of terrain and measurement of the structure and thickness of continental and floating ice.

Early results of the Nimbus one-month coverage, with three-mile resolution shows the breakup of tropical storm Cleo on consecutive days (August 29 and August 30, 1964) over the United States.

Figure 5.2 shows extensive cloud formation over the Alps and central Europe as revealed by infrared photographs taken at midnight from an altitude of some 275 miles. This photograph illustrates the fact that temperature generally drops as a function of height. The darkest areas are the relatively warm bodies of water, the lighter, i.e., cooler areas are land masses, the still-lighter areas are mountains within these masses and the lightest are clouds, whose shade varies from light gray to white depending on altitude. These photographs can be used, in fact, to measure temperature differentials as small as $1^{\circ}K$. An IR photograph of the Antarctic continent and the South Indian Ocean, also taken at midnight, is shown in Figure 5.3. Here the bright mass surrounding the south pole illustrates the gradation in temperatures measurable in ice masses. The formations at the center are clouds breaking up into smaller cells at temperatures higher than those of the ice.

On its trip to Mars, Mariner 2 provided the first measurement of the albedo of the earth--the ratio of reflected to incident light-viewed from space. Until Mariner 2, photometric studies of earthlight were based primarily on the secondary reflection of this light from the moon. These studies led to the conclusion that the earth albedo varies seasonally from 0.52 in October to 0.32 in July, with a mean value of 0.36. The fact that the navigation system of Mariner 2 required optical tracking of the earth by an instrument which at the same time provided a measurement of the intensity of light received has allowed a check of the albedo. Over 52 days, from September 29 to November 22, 1962, sufficient photometric data was telemetered by Mariner 2 to permit an independent calculation. The results have verified those previously obtained. In addition, the Tiros

program has permitted exact measurement of the variation in albedo as a function of terrain, based on fine analysis of more than 10, 000 Tiros photographs.

Bibliography

1. R. L. Wildey, "Photometry of the Earth from Mariner 2," J. Geophys. Res., 69 (1 Nov 1964), 4661.

2. A. Danjon, "Albedo, Color, and Polarization of the Earth," The Earth as a Planet, ed. G. P. Kuiper, Chicago, 1954, p. 734.

3. A. A. Arking, "Global Distribution of Earth Albedo and Cloud Cover," 236th National Meeting, American Meteorological Society, New York, January 26, 1965.

4. A. Schnaph, "Tiros I, II, and III -- Design and Performance," Aerospace Eng., 21 (June 1962), 42.

5. L. F. Hubert et al, "Estimating Maximum Winds in Hurricanes from Satellite Pictures," 236th National Meeting, American Meteorological Society, New York, January 26, 1965.

6. S. Fritz, "Research with Satellite Cloud Pictures, Astr. Aerosp. Eng., 1 (April 1963), 70.

7. C. H. B. Priestly, "The Width-Height Ratio of Large Convection Cells," Tellus, 14 (1962), 123.

8. A. J. Faller, "An Experimental Analogy to and Proposed Explanation of Hurricane Spiral Bands," Proc., Second Technical Conference on Hurricanes, June 27, 1961. Miami, Fla.

9. W. Nordberg and H. Press, "The Nimbus 1 Meteorological Satellite," Bull. Amer. Met. Soc., 45 (Nov 1964), 684.

Figure 5.2   Infrared Photo over Alps
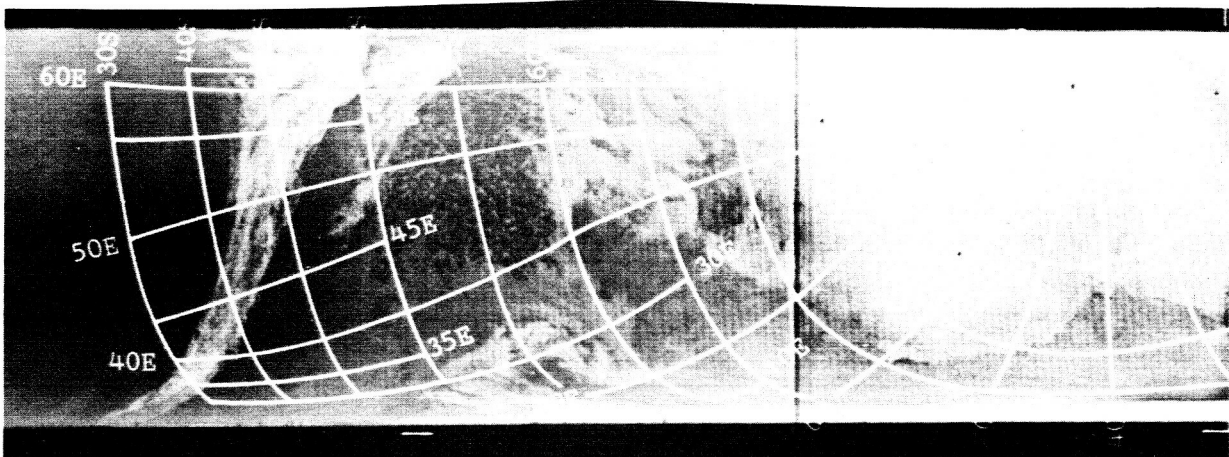
Figure 5.3   Infrared Photo over Antarctica

6. METEOROID ENVIRONMENT EXPERIMENTS

A discussion of meteoroid flux models was given in Reference 2.1, additional comments on the earth dust cloud are given in Appendix A to this report. A better definition of the meteoroid environment, both in the neighborhood of the planets and in the interplanetary space through which the manned vehicle will be traveling, is important because of present uncertainties in meteoroid flux and, equally as important, uncertainties in the velocity spectra of the meteoroids. The sensitivity analysis summarized in Figure 3.2 emphasized the relative importance of an improved knowledge of the meteoroid environment to the design of the manned vehicle planetary.

The problem of measuring the meteoroid environment in the particle mass range of interest is made difficult by the limited size of sensors that are capable of measuring particle velocity and direction as well as mass. Sensors of this type are usually limited to detector areas of fractions of a square foot, and the probability of encountering particles of milligram sizes, which tend to size the manned system shielding, are remote. The other approach to the problem is the use of Pegasus-type vehicles, which have relatively large detector surfaces, but are unable to sense particle velocities, which are essential to the design of shielding.

Two approaches have been taken by TRW to the meteoroid environment sensing problem: the first is the use of relatively small sensors that have the capability to measure particle masses and velocities and are suitable for use on Voyager-type satellites; and second, is the use of meteoroid flash detectors onboard spacecraft orbiting about Mars. These latter detectors were proposed by Dr. S. Altshuler at TRW, and are presently under evaluation by NASA. A description of these sensors is given in Reference 6.1. Conventional sensors capable of measuring particle masses, velocities, and compositions are described in the following paragraphs.

Sensors of the type shown in Figure 6.1 have a narrow cone angle of detection, and will be mounted on the spacecraft in the following manner:

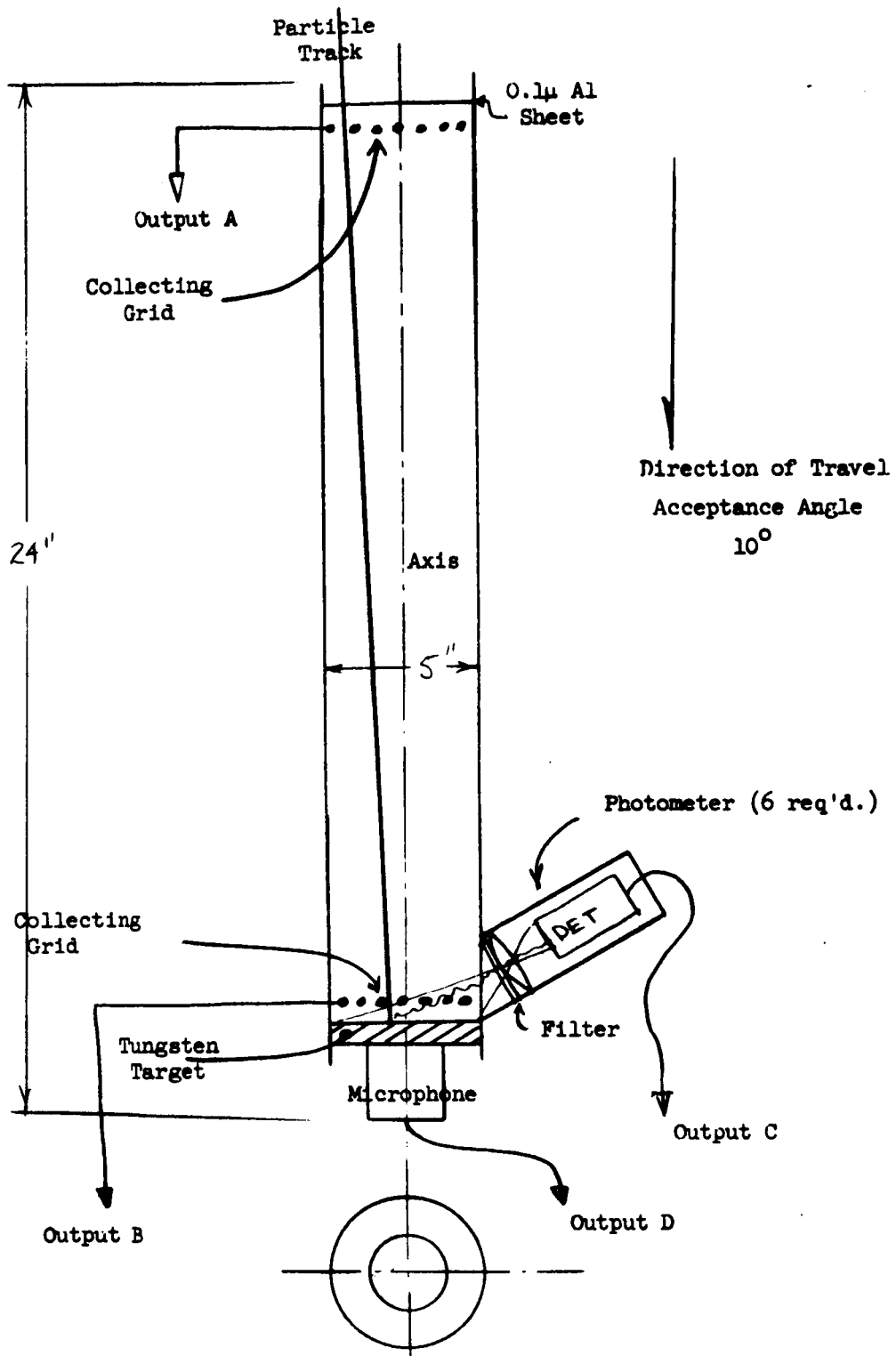6.1 F. N. Mastrup, "Meteoritic Analysis." 8 June 1965.

Particle Track

0.1μ Al Sheet

Output A

Collecting Grid

24"

Axis

5"

Direction of Travel
Acceptance Angle
10°

Photometer (6 req'd.)

DET

Collecting Grid

Filter

Tungsten Target

Microphone

Output B

Output C

Output D

Figure 6.1   Narrow Cone Angle Meteoroid Sensor

1. $\vec{Sun}$ x $\vec{Canopus}$

2. $\vec{Sun}$

3. $\vec{Canopus}$

4. - $\vec{Sun}$

It is expected that the average of all detectors will be about one count in 10 days per detector in interplanetary space and about one count in 10 seconds per detector in orbit around Mars. Time of flight will be measured between pulses A and B and converted to a digital count. Filter spectrometry of the impact flashes is included to evaluate energy and composition of the meteorites, and is employed to analyze the ionized products of hypervelocity impact. This involves analyzing the signal received at C.

Sensors of the type shown in Figure 6.2 will be mounted on the spacecraft with orientations similar to those for the sensors of Figure 6.1. It is expected that the average of all detectors will be about one count per day per detector in interplanetary space and about one count per second in orbit around Mars.

Filter spectrometry of the impact flashes will be used as before to evaluate the energy and composition of the meteorites.

Each sensor requires about 1 watt of power. The relative weights and volumes of each sensor are given in the following table.

	Narrow Cone Sensor	Wide Cone Sensor
Weight (lbs)	5.5	4.0
Detector	(1.5)	(2.0)
Signal Circuitry	(2.0)	(1.0)
Power Supply	(2.0)	(1.0)
Volume (in^3)		
Electronics	48	48
Power Supply	24	24
Sensor	(see sketch)	(see sketch)
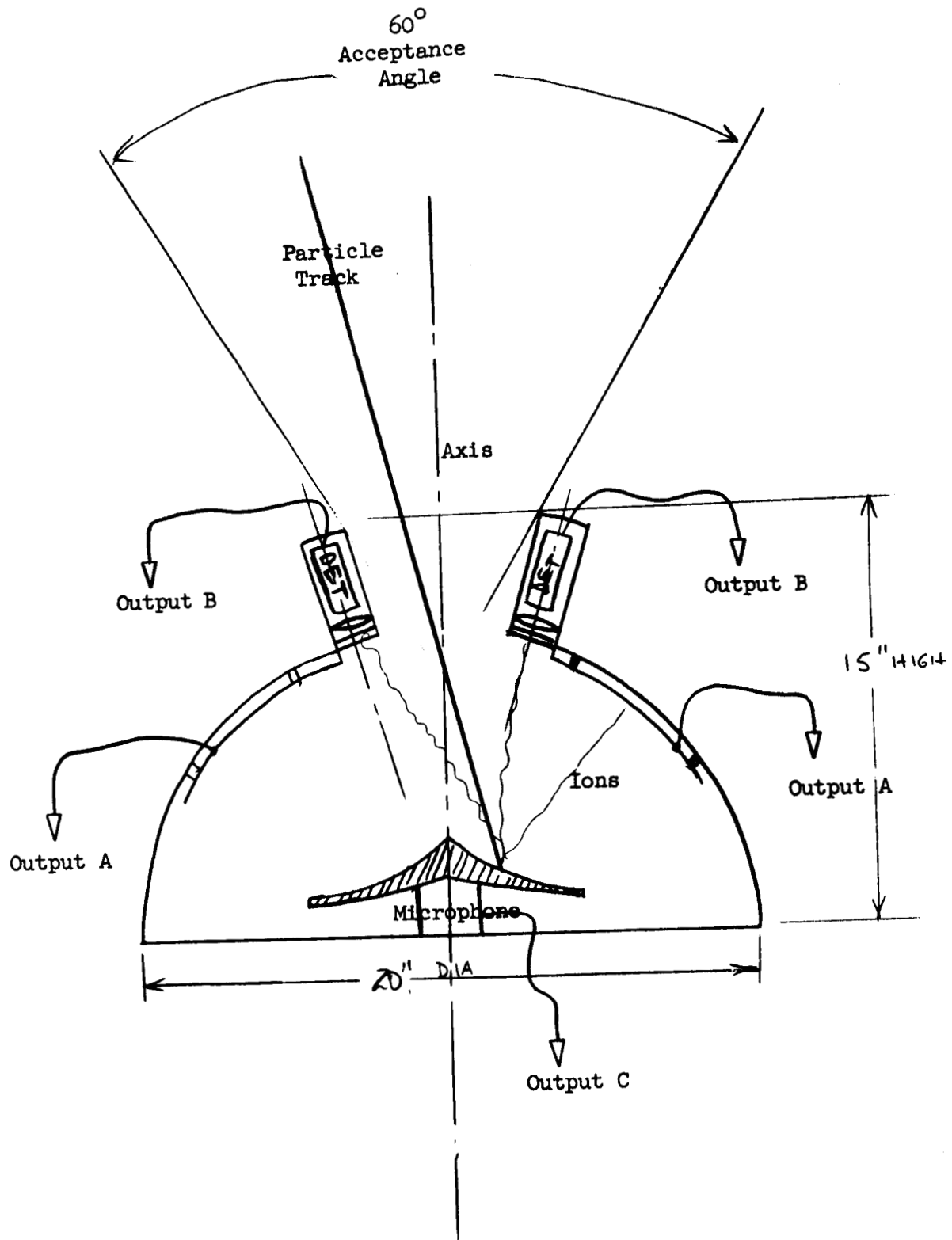
Figure 6. 2   Wide Cone Angle Meteoroid Sensor

7. MEASUREMENTS OF THE ATMOSPHERE

One of the most difficult elements of the Martian environment to measure satisfactorily is the atmosphere. Consideration of this problem leads to the realization that accurate definition of the atmosphere may be more difficult than is presently realized. The results of the Mariner IV occultation experiment and of more recent IR spectrometric measurements made from Earth-based observatories indicate that the surface pressure of Mars is much closer to the Model 2 (25 mb) or Model 3 (10 mb) values than to the 132 mb upper limit considered in the present study. Although this fact in itself does not pose questions of feasibility for aerodynamic braking within the Martian atmosphere, the Mariner IV occultation experiment indicates the possibility of still lower surface pressures ($<$ 10 mb). This finding, if verified, would pose serious questions as to the feasibility of aerodynamic deceleration within the atmosphere, both for capture of the main spacecraft, and for landing of excursion modules. The difficulty at present lies in the discrepancy between the surface density as measured by Earth-based IR spectroscopy, and the flyby occultation experiment. The resolution of these differences may require additional experiments, and possibly the use of aero entry capsules. Several available experimental techniques are discussed in the following section in terms of information obtained about the atmosphere (pressure, density, constituents, scale height), spacecraft modes required, and possible uncertainties in conclusions drawn from the measurements.

7.1 Earth-Based IR Spectroscopy

A brief review of experiments in the IR spectroscopy area is given to serve as a basis for our present understanding of the Martian atmosphere. A note by Spinrad (Reference 7.1), describing IR spectrometric experiments by Spinrad, Münch and Kaplan, is summarized below.[1]

Spinrad remarks that the thin atmosphere of Mars makes the detection of its constituents by Earth-based spectroscopic means a difficult task, however, one which has many possibilities for establishing at least the amount of carbon dioxide in the Martian atmosphere, and also the level of the surface density.

---

1. See Reference 5.2, Volume I.

"The polyatomic constituents of the atmosphere absorb best in the infrared where our detectors are least sensitive. . . however, these molecules do absorb sunlight weakly in the near-infrared and red where detectors are better and suitable spectrographic equipment is available. . .

"There are only two positively identified gases in the Martian atmosphere. In 1948 Kuiper detected small absorptions at 1.6μ and 2.0μ which are due to CO_2 on Mars. These Martian absorption bands are super-imposed upon the weaker telluric bands of carbon dioxide. The second gas detected was water vapor; in April 1963, Spinrad, Münch and Kaplan found some eleven weak Doppler-shifted Martian H_2) lines near 8200 on a high dispersion spectrogram, taken with the Mount Wilson 100-inch reflector. . .

"Most of the determinations of the absolute amounts of both CO_2 and H_2O in the Martian atmosphere are dependent upon the total gas pressure at the surface of Mars. Previous estimates for the CO_2 abundance, for example, vary from two to thirty times the amount above a unit area on earth - depending on how the pressure correction was made and what surface pressure was assumed. The reason for the pressure term in the Martian abundances is as follows: The shape of an individual planetary absorption line in a molecular band depends on the prevailing temperature which governs the Doppler width of the line, and the number and kinds of molecular collisions per unit time which determine the so-called Lorentz width. The Lorentz width is mainly dependent on pressure - and the dependence upon pressure is linear. Now the relationship between the strength of an absorption line and number of absorbing molecules necessary to produce it is a somewhat complex function called the curve of growth. For very weak absorptions, the number of absorbing molecules is directly proportional to the measured amount of absorption - hence, this part of the curve of growth is called the linear region. When the absorption is stronger, so that the line becomes very deep at its center, it becomes 'saturated.' That is, as more molecules are poured into the absorbing column, the absorption line grows at a slower rate than the increase in the number of absorbers would suggest. The rate of increase of absorption depends mostly on the line width - and thus on the pressure.

"Now if we are fortunate enough to have observations of several weak and strong bands of CO_2 in the Martian atmosphere, then we can use the curve

of growth to establish both the amount of carbon dioxide (from the linear part of the curve) and the total surface pressure from the observations on the strength of CO_2 bands lying on the saturated part of the curve of growth.

"One afternoon we decided to look at the Mars spectrum near λ 8700 - the $5 \nu_3$ band of CO_2 is visible on Venus there. We expected nothing, for the accepted amount of CO_2 on Mars was so small compared to that estimated for Venus that no CO_2 lines in this band should have been noticed, even with our high spectral resolution. Well, of course, the unexpected often happens in Astronomy - we could easily see the R-branch and some of the P-branch lines in this CO_2 band on Mars in the microscope.

"We have since measured the CO_2 line strengths in this resolved band; unfortunately, the rotational lines are really very weak ($\sim$ 4m$\overset{o}{A}$ at maximum) and the resulting measurements are probably not very accurate. These lines are on the simple linear part of the curve of growth, and thus with another valuable laboratory calibration by Dr. Rank, we decided that the atmosphere of Mars contains about 70 meter-atmospheres of CO_2. That is about 27 times as much as over a unit area on Earth. Thus, the curve of growth is anchored at the linear section. Now the determination of the surface pressure employs the published observations of Kuiper (1952) and Sinton (1963) for the CO_2 bands between 1 and 2 μ in the saturated regime. There is no place for all the details here, but we may approximate the surface pressure determination in the following way: for a band on the linear part of the curve of growth, the band strength W_1 is proportional to the amount of CO_2, m_1.

$$(1) \quad W_1 \sim m_1$$

and for a stronger band which is partly saturated, the band strength W_2 will depend upon the product of the amount m_2 and the pressure, P.

$$(2) \quad W_2 \sim (m_2 P)^{1/2}$$

and since $m_1 = m_2$ because the actual amount of CO_2 is the same in either equation, we can solve for P if W_1 and W_2 are accurately measured, and the constants of proportionality known. This technique gives a resulting surface pressure of some 30 mb, and detailed work including self-broadening and

temperature corrections move the pressure down to some 20 mb. The details of the computation are currently in progress, most of the work being done by Dr. L. D. Kaplan. We consider the estimate of 20 mb good to a factor two. The older polarimetric determination of the Martian surface pressure ($\sim$85 mb) may be suspect due to particulate scattering added to the assumed Rayleigh scattering by molecules.

"If the Martian surface pressure is really this low, then CO_2 becomes a major constituent. The partial pressure of 70 meter-atm. CO_2 on Mars is about 4 mb, and the CO_2 content by mass is then some $4/20 = 20\%$. What is the remainder? Not H_2O or O_2 - the amounts of these gases are very low ($<1\%$). The bulk of the rest is probably N_2 and A. Argon in the Earth's atmosphere has been radioactively generated in the crust from potassium -40. If Mars received the same percentage of K^{40} as had the Earth's crust, it should have enough argon to exert a partial pressure of 5 mb - or some 25% of the atmosphere by mass. By default and analogy to the Earth, the remaining 55% should be N_2. But the reader should be warned that this mixture rests on uncertain foundations. The method used to determine the amount of CO_2 and the surface pressure is probably excellent, but the observations need improvement by repetition. And this requires a large reflector with a modern Coude' spectrograph."

During the recent Mars-Earth opposition additional and more refined measurements of the Martian environment were made using the IR spectrometric technique described by Spinrad above. The results of these refined measurements have not yet been published, however, preliminary results indicate that the measurements are not significantly different than those published previously, that is, the surface pressures are still estimated to be approximately 20 mb, with the CO_2 constituent still comprising some 20% by mass of the overall atmosphere.

It should be noted that the technique described above for measuring the Martian atmosphere is limited to the direct measurement of the amount of CO_2, and cannot be used to verify the existence of the amount of nitrogen or argon present in the atmosphere. Hence, the general technique is limited in its ability to completely define the Mars atmosphere.

The problem of defining the amount of nitrogen and argon present in the Martian environment must be approached by other techniques, possibly by the use of UV spectrometers from spacecraft orbiting about the planet. The detection of nitrogen could be accomplished by a scattering experiment in the upper atmosphere of Mars, however, the scattering coefficients are not well known and significant uncertainties would exist in the amounts of nitrogen estimated based upon these measurements. Likewise, argon might be detected by UV spectrometers although significant uncertainties would exist in the amounts of argon estimated from these measurements. Hence, it does not appear possible to completely define the constituents in the Martian atmosphere using spectroscopy techniques alone, although the amount of CO_2 in the atmosphere, as well as the surface density, should be estimated within reasonable limits by this technique.

7.2 Flyby Radio-Occultation Experiments

The recent Mariner 4 mission utilized the principle that radio propagations through the Martian atmosphere changes the phase and frequency of the Doppler tracking signal to give indications of some of the physical properties of the atmosphere. The occultation experiment was proposed in the spring of 1964 and was subsequently accepted as an experiment on Mariner 4. The experiment required only a slight change in the planned orbit of the spacecraft about Mars such that sharp occultation of the RF signals would occur as the spacecraft passed behind the planet. The following description of the technique is taken from Reference 7.2.

"As the spacecraft approaches the occultation region, the presence of an ionosphere and atmosphere will first cause the velocity of propagation of the radio signal to change from that in free space, owing to the non-unity effective index of refraction of the ionospheric medium. Secondly, the radial gradient in the effective index of refraction will cause the radio beam to be refracted slightly from a straight line path. Both of these effects will cause the phase path of the signal at any time, t, to differ from what would be observed in the absence of an atmosphere and ionosphere by the amount,

$$\Delta r(t) = \int nds - R(t)$$

$$\Gamma(t)$$

where n = index of refraction, Γ (t) = actual path taken by the refracted ray from the tracking station on Earth to the spacecraft at time t, and R(t) = straightline path to the spacecraft at time t.

Thus, if the geometry of the spacecraft trajectory and the spatial characteristics of the index of refraction are known, the phase change can be computed readily. Conversely, if the geometry and the amount of phase change are known at any given time, the spatial characteristics of the index of refraction, and hence of the atmosphere and ionosphere, can be inferred by a process of inverting the above equation or by model-fitting. . .

"Deviations of the received Doppler from predictions based on orbit determination will be caused by atmospheric and ionospheric phase effects.

"The magnitude of these effects has been computed for a simple isothermal model atmosphere, having a surface pressure of 25 millibars, a scale height of 14 km."

The analyses indicate that these effects will not cause significant loss of meausrement accuracy for the purposes of defining surface density and scale height. The mean molecular weight can be estimated from the combination of the scale height and temperature, and this combined with the information about the refractivity at the surface will permit estimates to be made of the amounts of nitrogen and argon present when the absolute amount of CO_2 is assumed based upon the spectroscopic studies as described above. From this information it will be possible to estimate atmosphere density and pressure at all heights.

Since the refractivity is the sum of the refractivities of the various constituents and these latter refractivities are in turn directly proportional to the density of each constituent, the density of argon and nitrogen can then be estimated since the amount of CO_2 is well known from other observations. The amount of argon and nitrogen can be kept in proper proportions to produce the observed total refractivity. The sum of the three densities will then be the total atmospheric density. The density and temperature information lead to a knowledge of pressure as a function of heights.

It is noted in Section 5, Volume I, of the present report, that there is a possibility that an ionization layer will exist near the surface of Mars due primarily to the lack of an atmospheric constituent that can reabsorb electrons as molecules become ionized due to solar radiation. Recent analyses by TRW indicates that this will have a strong effect upon the results obtained by the occultation experiment described above depending upon the electron concentration within the surface ionization belt, and the atmosphere constituents that are available to absorb the produced electrons. The two possibilities indicated by the TRW analyses pertain to the amount of nitrogen and the amount of argon present in the atmosphere. The results indicate that if nitrogen is the only other major constituent in the Mars atmosphere a 10 percent error at most would be incurred in the surface pressure in the occultation experiment. In addition a solar event would have to be in progress at the time of the occultation experiment in order to induce erros of this magnitude. There would also be a tendency to overestimate the scale height by approximately the same amount if nitrogen is the other major constituent in the atmosphere.

The results are greatly different if argon is the other major constituent in the Mars atmosphere. In this case, an error that is several times the magnitude of the indicated pressure is induced because the electron densities in the case of an Argon-CO_2 atmosphere are much greater than in the case of the Nitrogen-CO_2 atmosphere. Furthermore, this large error in the occultation experiment will be present even in the absence of solar events. Although the presence of Argon in the Martian atmosphere is strictly speculative at this time, its presence could induce very large errors in the occultation experiment, to the point where the results obtained with the occultation experiment are not realistic. In actuality, the major constituents in the Mars atmosphere may be nearly equal proportions of Argon and Nitrogen in combination with the CO_2. In this case the possible errors introduced into the occultation experiment will be somewhat reduced but will still be significant.

In summary, the occultation experiment is an extremely useful and effective technique for defining the surface pressures and scale heights in the Martian atmosphere, provided Argon is not present in substantial amounts.

In view of the fact that the amount of Argon in the Martian atmosphere is not known, the accuracies or uncertainties introduced into the occultation experiment likewise are not known at the present time. In addition, the amount of Argon (and Nitrogen as well) is extremely difficult to determine by spacecraft that do not enter the Martian atmosphere, hence, the uncertainty in the occultation experiment may be very difficult to eliminate.

Uncertainties in the occulation experiment can be removed by other means, because the effects of the surface ionization layer upon the occultation experiment are dependent upon the frequency of the radio propagation. The Mariner 4 experiment was conducted at about 2.3 kmc, and no attempt was made to repeat the experiment at other frequencies. However, since the effect of the surface ionization layer is dependent upon the frequency of the radio propagation, an occultation experiment could be performed where two frequencies are used, suitably separated so that the effects of the surface ionization layer on the phase and amplitude of the propagated signals can be resolved. In this manner a reasonably accurate determination of the effect of the surface ionization layer can be made and suitable allowances made. It should be emphasized, however, that this experiment is still an indirect measurement of the atmosphere and will not give a conclusive indication of all constituents in the atmosphere.

7.3 Entry Capsule Experiments

Several investigators have suggested the use of a small light weight entry capsule into the Mars atmosphere to measure the density and possibly the major constituents in the Martian atmosphere. Clearly this direct measurement of the density and scale height of the atmosphere is desirable and will yield accurate results for engineering purposes. As suggested by Seiff and others (Reference 7.3), spectroscopic analyses also can be made of the shock wave surrounding the entry capsule to get an indication of the constituents in the Martian atmosphere. As Seiff points out:

"It is fundamental to gaseous radiation that a spectrum consists of bands, lines, and continua which are characteristic of the gases involved. Measurement of the intensities of selected bands as functions of velocity and free stream density during entry can, therefore, provide data on the presence or absence of selected constituent gases . . .

"The primary candidate experiment of this kind for the Mars atmospheric probe is the measurement of the presence of nitrogen (as yet only <u>assumed</u> to be a principal constituent of the Mars atmosphere) and its mole fraction. This can be accomplished by measuring the intensity history of the prominent cyanogen violet band system. These bands are now well known to be responsible for the very high levels of luminous intensity associated with nitrogen and carbon dioxide mixtures . . .

"Given the free stream conditions, and a gaseous atmosphere consisting primarily of nitrogen and carbon dioxide, the measurement of CN violet intensity can be used to define the proportions of N_2 and CO_2, except for an ambiguity that arises because the curve is double valued. However, for any given pair of gas mixtures, this ambiguity occurs at one velocity only . . . Thus, from radiometric measurements of the intensity of the CN violet system as a function of time during entry, the presence of nitrogen can be determined, and its mole fraction established.

Additional radiometers sensing the NO gamma bands, the C_2 Swan bands, and the N_2^+ (1-) provide additional checks on the interpretation of the CN violet radiometer. Thus, if the readings of these instruments are not consistent with those expected from CO_2 - N_2 mixtures, it is implied that other gaseous constituents are present in important amounts. For example, the presence of nitrogen oxides in the atmosphere would enhance the NO system. Argon increases the shock layer temperature at a given speed, and shifts the peak intensity of the CN system to a lower velocity."

It is noted in the above discussion that the amount of argon in the Martian atmosphere, if present, will be determined by indirect measurements involving the shift in peak intensity of the CN constituent. In view of the fact that large amounts of Argon may be present, whereas the above experiment is designed primarily to measure the Nitrogen constituent along with the known CO_2 content, the experiment may not yield satisfactory determinations of the amount of Argon in the atmosphere. However, the experiment would be an extremely valuable one in any case.

7.4   Lander Experiments on the Surface of Mars

The final experimental technique to define the Martian atmosphere is one that could be conducted on the Martian surface by a surviving lander payload. By far the most effective means of determining the atmosphere constituents in a spacecraft of this type is the use of a mass spectrometer which would sample the Martian atmosphere and determine the relative amounts of the various constituents present. This experiment could be conducted with a high degree of accuracy, it is a direct experiment rather than an indirect experiment, and could determine all of the gas constituents present and not only one or two of the principal constituents. It would seem that an experiment of this type would be highly desirable and should be performed as early as possible in the precursor mission programs. The surface pressure and temperature could be determined accurately with simple instruments and used as a basis for extrapolating the properties of the atmosphere to altitude based upon the performance of the entry capsule or lander as it decelerates through the Martian atmosphere. (The mixture of gases could be expected to be fairly constant throughout the sensible atmosphere.) In view of the fact that a mass spectrometer weighs something less than 10 lbs and requires small amounts of power, it would seem to be a highly efficient and useful experiment that ultimately will be required regardless of prior experiments based upon either flyby/orbiter spacecraft or those performed from nonsurviving entry capsules.

In summary, it can be seen that many of the experiments that can be conducted from flyby/orbiter spacecraft to determine the properties of the Martian atmosphere yield data that are little better than that obtainable from the Earth-based stations using IR spectroscopy. The next experiment of significance is that which can be performed from an entry capsule to determine the density and scale height properties to a satisfactory degree of accuracy, but may not be entirely satisfactory to determine the relative amounts of constituents in the atmosphere. By far the most satisfactory experiment is that carried out by a mass spectrometer and state measurement instruments from a lander spacecraft. Hence, an early attempt should be made to perform a minimal early lander mission.

8. CONCLUSIONS

The following conclusions can be drawn from the results presented herein:

1. The priorities for the experiments in the order of their importance are: solar cosmic radiation environment, meteoroid environment, and atmospheric properties.

2. A numerical rating system for the experiment priorities is difficult to establish because basically different factors dictate the selection of the experiments, some based on design feasibility which tends to be either positive or negative without numerical differentiation, and others which are amenable to quantitative evaluation because bounds can be placed on the environmental factors involved and weight penalties estimated for design modifications necessary to accommodate the uncertainties. If bounds can be placed on the uncertainties, priorities generally can be reduced.

3. A comprehensive experiment program should be performed in earth-based facilities to establish shielding effectiveness and man's tolerance to the solar radiation environment.

4. A basically new approach to the measurement of the meteoroid environment must be established in order to acquire meaningful data for shielding design criteria. The approach to the measurement of the meteoroid environment proposed by TRW can yield data on the masses, velocities, and heliocentric trajectory characteristics of the particles, for sizes of particles applicable to the design of the manned system. This approach should be explored for application to precursor missions.

5. Measurement of the Martian atmosphere, to an adequate degree of confidence, cannot be accomplished with indirect experiments using spectroscopic or radio occultation techniques. A minimum entry capsule should be deployed into the atmosphere on an early flight to determine density and scale height properties with acceptable confidence. A surface lander experiment is desirable to determine atmosphere constituents.

6. Meteorological experiments appear to be marginally rewarding to the design of the manned system when compared to the large amount of data that must be gathered and transmitted to the Earth which will impose penalties on the communications systems of the precursor vehicles. Careful consideration must be given to the scope of meteorological experiments to establish realistic mission goals.

7. Although television mapping of the planet is very important for establishing landing sites for the manned mission and to support the bio-contamination and other scientific experiments, the communication requirements to support the TV mapping experiments are extremely large and must be realistically limited in order not to place excessive requirements on the unmanned precursor missions. Selection detailed TV mapping should be planned to complement the coarse-resolution comprehensive coverage.

8. Surface properties measurements from a single lander are not entirely adequate. Landers must be equipped with TV systems (for coverage during and after descent) to permit " extrapolation" of surface properties measurements to at least the immediate surroundings. Multiple landers, augmented by low altitude orbital mappers, are desirable. A very effective surface properties experiment can be accomplished with an instrumented surface rover, whose performance is directly affected by surface properties. Much greater area coverage can be achieved by this technique.

APPENDIX A

METEOROID ENVIRONMENT IN THE VICINITY OF EARTH AND MARS

A.1 Meteoroid Flux Near the Earth

The two primary sources of meteoroid flux data near the Earth are the following:

1. Visual and radar tracking of meteoroid trails as the particles graze the upper atmosphere at high velocities. The data thus obtained are particularly valuable because particle velocity and flight direction can be determined with good accuracy by triangulation techniques from ground stations. Particle mass is computed by noting the visual magnitude of the particle trace. Particle sizes thus noted range from about milligram to gram magnitude. Several thousand measurements have been made to date.

2. Satellite observations using primarily microphone and solid state detectors. Measurements made in this manner apply to micrometeoroid particles, ranging from 10^{-7} to 10^{-12} grams in size. Data thus obtained are much less satisfactory than that from ground stations for several reasons. First, particle velocities and flight directions are not measured, hence, the source of the particles cannot be determined. The data obtained are indications only of the kinetic energies of the particles (by the ionization generated at impact), from which particle mass and flux rate must be estimated by assuming an average velocity. Neither is it possible to derive the velocity spectrum of impinging particles, as it is from the ground based observations. The small area of the detector constitutes a further limitation, which makes it unlikely that relatively large size particles (milligram and larger) will be encountered. This latter problem is important from the standpoint of manned planetary vehicle design, because milligram-size particles can be encountered during the course of year-long missions. (The Pegasus meteoroid-detector satellite has adequate detector area for this purpose, but is experiencing detector difficulties caused by operation in the trapped radiation belt.

A summary of the meteoroid flux data obtained from the above sources is presented in Figure 1. Whipple[1] has developed a flux-mass law for the visual-radar meteoroid data, assuming a correlation between the observed visual magnitudes and particle mass. The resulting law is

$$N = 1.34 \ln m + 14.34 \ (particles/cm^2/sec)$$

This law can be seen to intersect the earth satellite data at particle sizes of about 10^{-9} grams. An extrapolation of the Baker law falls below the earth satellite data by about three orders of magnitude.

The earth satellite data generally has a much steeper flux-mass characteristic, in the micrometeoroid region from 10^{-7} to 10^{-12} grams, giving rise to the belief that a "dust cloud" surrounds the Earth.

Although the nature and extent of such a dust cloud is not known with certainty, Whipple[1] has cited some data that indicate a strong variation of dust cloud flux with altitude (see Figure 1). At a mass of 10^{-9} grams, the flux is estimated to drop off by over four orders of magnitude from low altitude to high altitude. It was noted previously that Mariner II data (which is based on a few hits only, obtained in interplanetary space) falls near the lower extremity of the curve. Although additional data are needed to verify the nature of the dust cloud, it is of interest to hypothesize a source, or sources, for the dust cloud. In particular, the contribution and nature of aerodynamic capture of meteoroids are analyzed.
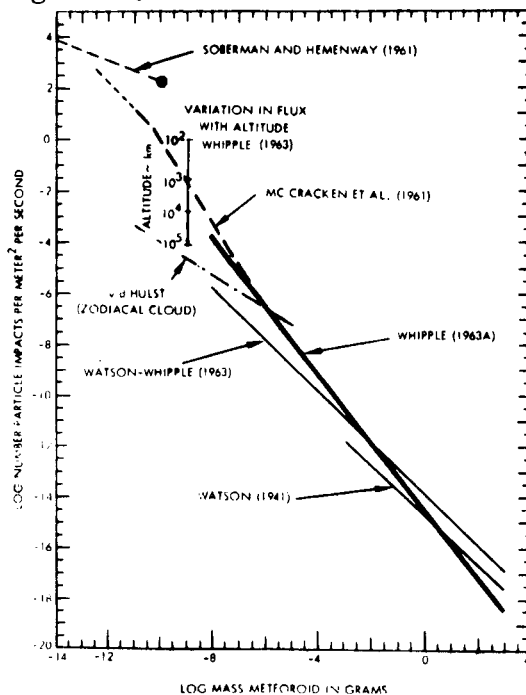

Figure 1. Meteoroid Flux Models

1. F. L. Whipple, "On Meteoroids and Penetration."
   AAS Preprint 63-29. January 15-17, 1963. Los Angeles

A. 2   Aerodynamic Capture of Micrometeoroids

The purpose of this discussion is to demonstrate the effectiveness of aero-
dynamic capture of meteoroids, and particularly micrometeoroids.   This
phenomenon has not been examined in detail, but appears to be a likely source
of the dust cloud around the Earth.   If aerodynamic capture is an effective
meteoroid trapping mechanism at Earth, it can also be expected to give rise to
a similar phenomenon at Mars and Venus.   In addition, by extracting energy from
meteoroids that graze the upper atmosphere, but escape capture, the paths of many
meteoroids in interplanetary space will become similar to that of the encountered
planet, so that annualar dust rings may be generated which circle the sun with
orbits similar to that of the planet.   An analysis and computations are presented
herein to demonstrate these possibilities.

Consider a meteoroid
approaching the Earth from
interplanetary space, with a
remote velocity, V_o, with
respect to the Earth.   The
particle will be deflected
from its heliocentric path
by the gravity field of the
Earth by an amount depend-
ing upon its remote velocity
and miss distance, b, with
respect to the Earth.   As
shown in Figure 2, the
particle will pass the Earth
at a perigee distance, g,
after an angle turn through
of 90° - θ .

A number of particles
can be expected to graze the
upper atmosphere, but
escape into interplanetary
space.   The paths of these
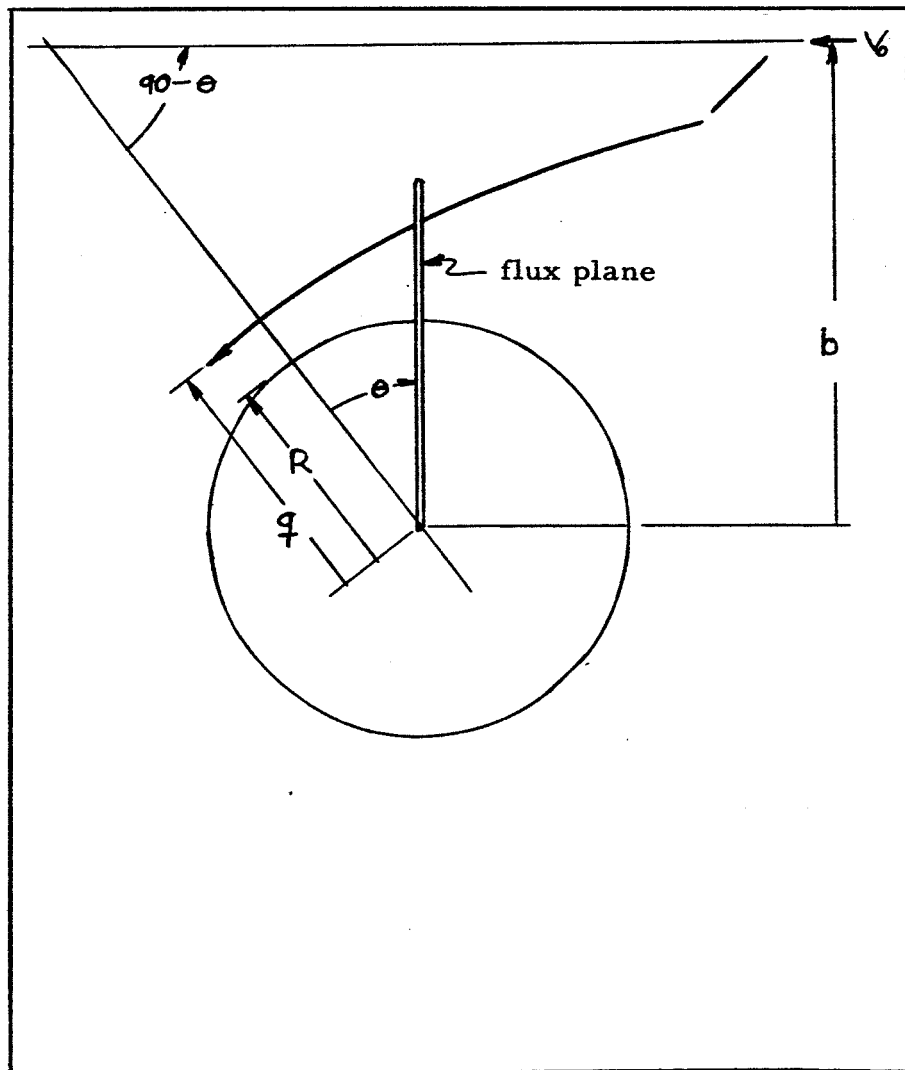hyperbolic particles will

Figure 2.   Aerodynamic Capture of Meteoroids

A-3

be different from those along which the particle approached, and their helio-centric orbits will be made more nearly circular, with reduced characteristic velocities. A consequence of this grazing maneuver will be an increase in the number of particles whose heliocentric orbits approximate that of the Earth (or the particular planet encountered).

Other approaching particles will plunge into the atmosphere of the planet and vaporize or fall to the surface before completing an orbit about the planet.

The remaining particles will enter a narrow corridor and decelerate into capture orbits about the planet. The lifetimes of the captured particles will depend upon the remote speed of approach, and upon the relative amount of energy removed on the initial pass. Hence, those particles that have approach speeds slightly above capture speed, and pass along the upper boundary of the corridor so that a small amount of energy is removed from the particle, can be expected to have relatively long lifetimes.

The upper and lower limits of the capture corridors are determined by:

1. The remote approach velocity
2. The ballistic coefficient of the particle, $W/C_D A$
3. The properties of the atmosphere

The diameter and mass of the planet also shape the corridor, although second order effects in these parameters can be ignored in the present analysis.

Maday in Reference 2 gives a correlation for the velocity ratio of a particle passing through a corridor. The upper corridor is that along which a particle is decelerated to escape velocity, or parabolic velocity; similarly, the lower corridor is defined as that along which a particle is decelerated to circular velocity. The relation for the velocity ratio along the grazing pass is (Maday's Equation (16)):

$$\frac{V_2}{V_1} = \exp\left\{ -B\rho_o \left[2\pi q (e+1)/\alpha e\right]^{1/2}\right\} \tag{1}$$

2. C. J. Maday, "Grazing Trajectories and Capture of a Ballistic Vehicle." AAS Symposium on Post Apollo Space Exploration. Chicago. May 1965

where

V_1 = velocity prior to deceleration

V_2 = velocity after deceleration

B = ballistic coefficient

= $C_D A/2m$

m = mass of particle, slugs

ρ_o = density of the atmosphere at perigee, slugs/cu ft

q = perigee radius, ft

α = lapse rate, 1/ft

e = eccentricity of the approach orbit

The above equation was derived on the basis of a small central angle turn through, and is accurate to within 1 percent for e = 1.5, and to within 10 percent for e = 9.0. Because the particles of interest to the present analysis have relatively low eccentricities, Equation (1) is considered sufficiently accurate.

The corridor boundaries can be determined by noting that:

$$V_1 = V_c (e + 1)^{1/2} \tag{2}$$

where V_c is the circular velocity.

By setting $V_2 = V_c$, the lower corrider is given by:

$$\left(\rho \sqrt{q/\alpha} \right)_l = \frac{1}{B} \sqrt{\frac{1}{8\pi} \frac{e}{e+1}} \ln(e+1) \tag{3}$$

Since escape velocity is equal to the circular velocity times $\sqrt{2}$, the upper boundary of the corridor is given by:

$$\left(\rho \sqrt{q/\alpha} \right)_u = \frac{1}{B} \sqrt{\frac{1}{8\pi} \frac{e}{e+1}} \ln \left(\frac{e+1}{2} \right) \tag{4}$$

A sketch of the corridor is given in Figure 3.

The functions on the left-hand side of Equations (3) and (4) are functions of altitude, and can be generated for any given model in Figure 4. The 1959 ARDC Model Atmosphere was used in the present analysis. Various values of eccentricity were assumed, and corridor boundaries computed for nominal values of ballistic coeffic ent, B.

Particles within the corridor will be moving at the following velocities:

Figure 3. Corridor Boundaries (at perigee)

Figure 4. Corridor Functions vs Altitude
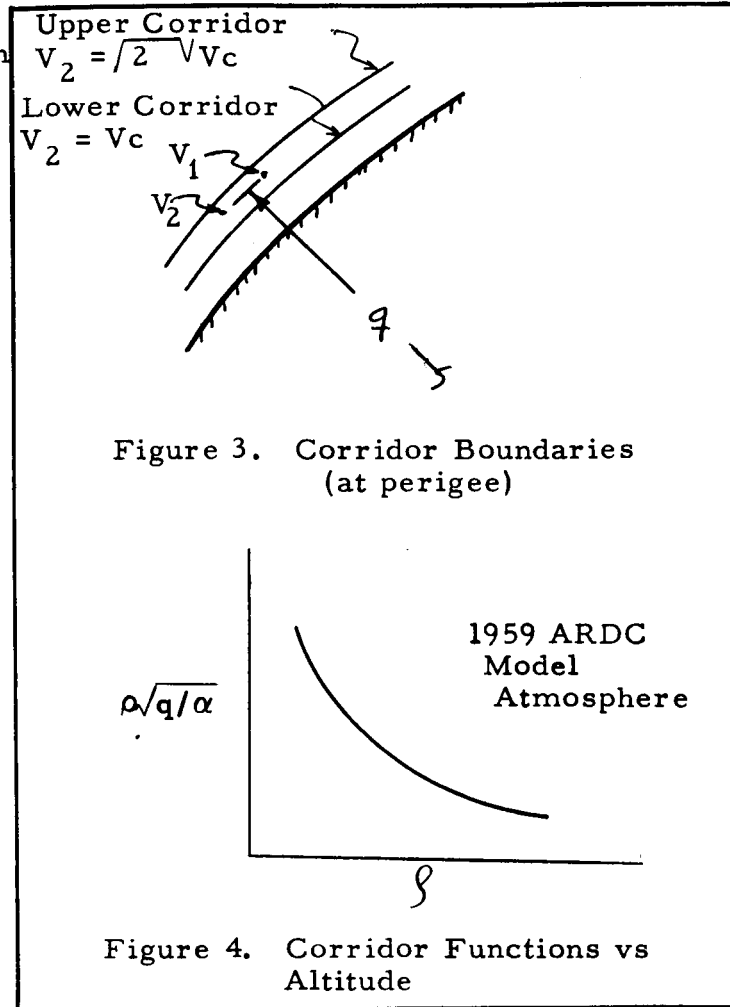
$$V_o = \sqrt{\frac{GM}{q} (e - 1)} \qquad (5)$$

$$V_1 = \sqrt{\frac{GM}{q} (e + 1)} \qquad (6)$$

$$V_2 = V_1 \left| \frac{V_2}{V_1} \right| \qquad (7)$$

where GM is the gravitational constant of the planet, and the ratio V_2/V_1 is given by Equation (1).

Particles within the corridor will go into capture orbits about the planet and eventually spiral to the surface. The lifetime characteristics of each particle is determined by:

A-6

1.   The starting conditions, V_2 and q

2.   The ballistic coefficient, B

3.   The properties of the atmosphere, ρ and α

The TRW lifetime program has been used to compute the number and characteristics of the decay orbits of the captured particles. A complete description of this program is given in Reference 3.

A. 3   Computation of Captured Flux Rates

The geometry of the capture corridor is influenced strongly by the remote approach velocities of the particles, which range from slightly hyperbolic values to near heliocentric escape values (140,000 fps). In order to develop a representative flux model it is necessary to account for the wide spectrum of approach velocities of the particles.

Lovell (Reference 4) reports velocity distributions for a large number of meteoroids observed by visual and radar techniques from ground-based stations. By assuming a velocity spectrum for meteoroids in free space near the Earth and transforming the spectrum into Earth-centered coordinates, reasonably good agreement was obtained with observed velocity distributions. The following assumptions were made about the velocities of the free space meteoroids:

1.   Few particles have heliocentric velocities of 30 km/sec; the majority have velocities of 36 to 42 km/sec.

2.   More particles move in the same direction as the Earth; fewer particles have retrograde orbits.

3.   T. Sands, "A Guide to the Satellite Lifetime Program".
Space Technology Laboratories, 9861.3-304, 27 February 1964

4.   Lovell, Meteor Astronomy, Oxford Press. 1954. p 242-246.

Based upon these criteria the distribution curves shown in Figure 5 were assumed. The remote approach velocity with respect to the Earth is:
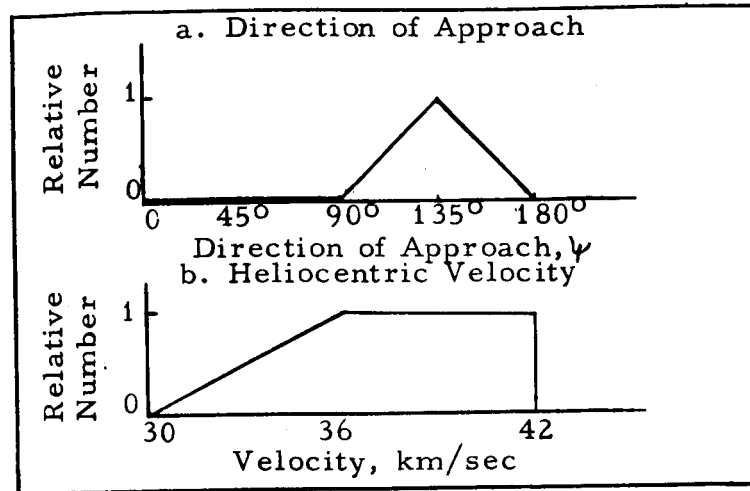

Figure 5 Velocity & Direction of Approach of Meteors

$$V_o = \sqrt{V_E^2 + 2 V_M \cos \Psi + V_M^2} \qquad (8)$$

where V_E is the velocity of the Earth and V_M is the heliocentric velocity of the meteoroid. Assuming the relative heliocentric distributions given in Figure 5, the velocity spectrum in the Earth coordinate system is given in Figure 6. Particle having zero velocity on this distribution are parabolic with respect to the Earth and pass the corridor perigee at escape velocity with respect to the Earth.

It is noted that the asymmetric approach angle distribution leads to a prediction of an asymmetric dust cloud about the Earth, which generally will take an ovate shape with the major portion of the swarm trailing the Earth. This effect will be investigated in more detail in a later phase of the analysis, for the present, the cloud will be assumed to be symmetric in the plane of the ecliptic. Also, consideration is not given to out-of-the ecliptic asymmetries.
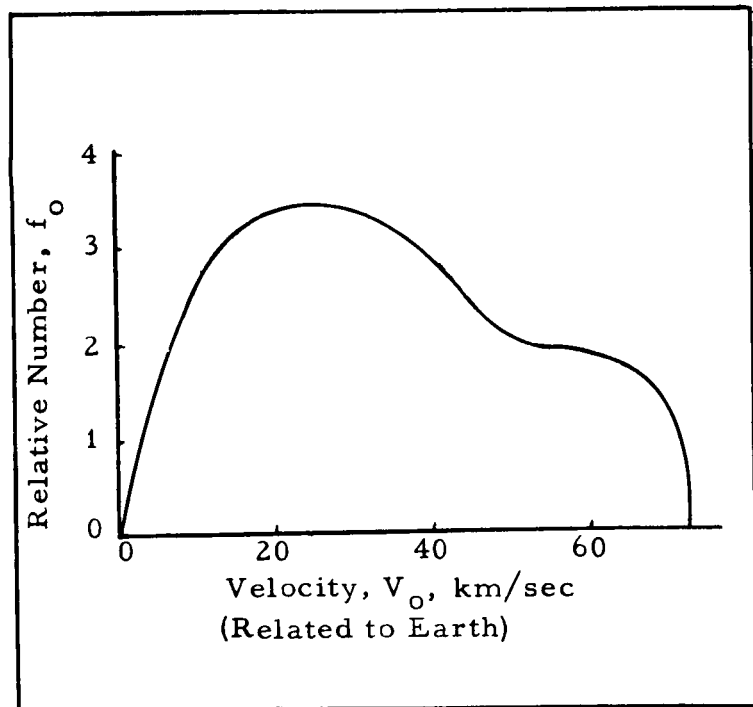

Figure 6 Meteoroid Velocity Distribution Relative to the Earth

Let f be defined as the number of meteoroids per mile of altitude approaching the Earth at a remote distance. If, for analysis purposes, we specify the eccentricity of the approach trajectory, e, the corridor dimensions can be determined from Equations (3) and (4), and the corresponding remote velocities, V_o, from Equation (5). The relative flux entering this corridor is given by the factor f_o, which is a function of approach velocity, V_o, as shown in Figure 6. The relative flux passing through the perigee of the corridor is given by:

$$f_p = f_o \frac{db}{dq}$$

$$= f \sqrt{\frac{e+1}{e-1}}$$

and the flux passing at any point along the capture orbit is given by:

$$f_c = f \frac{db}{dq} \frac{dq}{dr_f}$$

$$= f \sqrt{\frac{e+1}{e-1}} \left[\frac{1 + e_c \cos \theta}{1 + e_c} \right] \tag{9}$$

where e_c is the eccentricity of the orbit of the captured particle, r_f is the radius from the center of the Earth to the point in question, and θ is the true anomaly angle. The combination of e_c q_c, and θ determine the radius r_f, where q_c is the perigee of the captured particle. Curves of flux versus altitude can be generated from Equation (9) for a given swarm of particles in a decaying orbit for a given "look" angle θ. In actuality meteoroids will be approaching the Earth from all angles, hence, to account for all captured particles passing the flux plane (see Figure 4), it will be necessary to rotate the remote approach plane through an angle τ , and sum the contributions of all particles. This can be accomplished by assuming:

$$\theta = \theta_o + \delta$$

A-9

where δ is the angle of the remote approach plane with respect to the nominal, and is varied through ± 90 degrees. The entire process must be repeated for each group of particles in the velocity spectrum.

To the flux contributed by the captured particles, must be added the flux of the approach particles, which cross the flux plane during the initial grazing pass. For any given radius, r_f,

$$V_o = \sqrt{\frac{GM}{r_f} \; \frac{e^2 - 1}{1 + e \, Cos \, \theta}} \tag{10}$$

A corresponding value of f is given by $f(V_o)$ (see Figure 6). The flux contributed by the approach particles is:

$$f_a = f_o \left[\frac{1 + e \, Cos \, \theta}{\sqrt{e^2 - 1}} \right] \tag{11}$$

The angle θ must be varied over the allowable range of $\theta_o + \delta$. This allowable range is determined by:

$$\theta = Cos^{-1} - \frac{1}{e}$$

A comparison can now be made between the free space flux at any altitude and the sum of the approach flux captured flux to obtain an indication of the magnitude and altitude distribution of the dust cloud.

The process can be repeated for larger sized particles to determine the influence of particle size on dust cloud flux.

The results of an analysis of particles of mass 10^{-12} is shown in Figure 7. The relative flux contributed by the captured particles is 20 times that of the approach particles. The rapid decrease in captured particle flux with altitude is noticeable, and agrees with the variation hypothesized by Whipple up to altitudes of several thousand kilometers.

It was found that the flux contribution of the captured particles was dependent upon the flux-velocity distribution curve (Figure 6) in the neighborhood of the origin (as relative velocity goes to zero). Increasing the number of particles at near-parabolic velocities increases the number of captured particles markedly; the results shown in Figure 7 apply for a flux factor, f, of 0.2 at a relative velocity of zero.

It is interesting to note that the velocity spectra of the captured particles is shifted strongly to the lower velocities compared to that of the approach particles. Although computations have not been made to illustrate this effect, the implications for shielding design are evident.
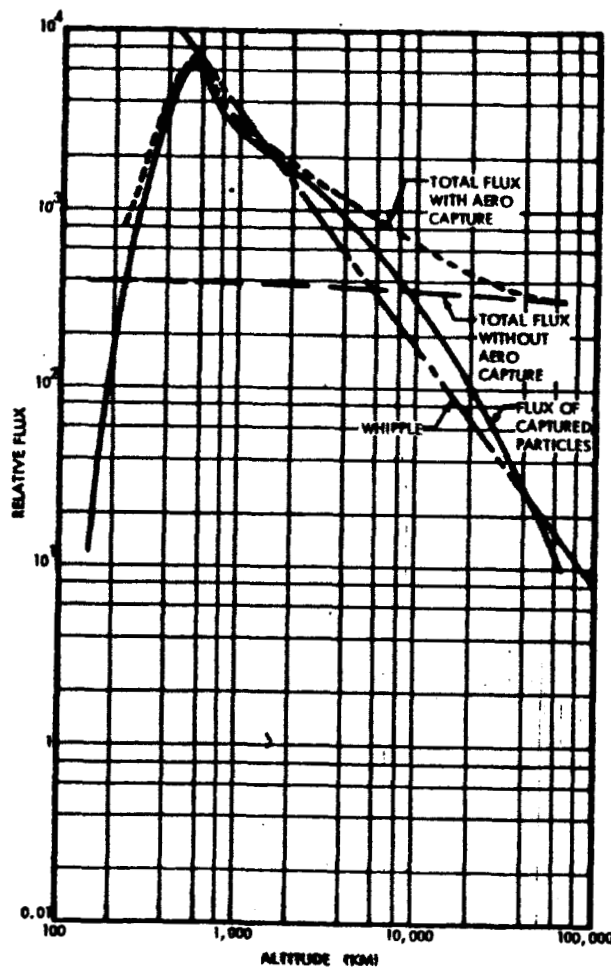

Figure 7. Effect of Aero Capture on Near-Earth Meteoroid Flux

A-11